5-1-2012

Assessment of field effect in the cancerous prostate

Christina Haaland

Christina M Haaland

Candidate

Biomedical Sciences, Biochemistry and Molecular Biology

Department

This dissertation is approved, and it is acceptable in quality and form for publication:

Approved by the Dissertation Committee:

Jeffrey Griffith, PhD　　, Chairperson

Marco Bisoffi, PhD

Robert Orlando, PhD

Eric Prosnitz, PhD

**ASSESSMENT OF FIELD EFFECT IN THE CANCEROUS
PROSTATE**

BY

CHRISTINA M HAALAND

A.S., Biotechnology, Seattle Community Colleges, 1999
B.S., Microbiology, University of Washington, 2001

DISSERTATION

Submitted in Partial Fulfillment of the
Requirements for the Degree of

**Doctor of Philosophy
Biomedical Sciences**

The University of New Mexico
Albuquerque, New Mexico

May, 2012

ACKNOWLEDGMENTS

Assessment of Field Effect in the Cancerous Prostate

by

Christina M. Haaland

A.S., Biotechnology, Seattle Community Colleges, 1999
B.S., Microbiology, University of Washington, 2001

Doctor of Philosophy, Biomedical Sciences

ABSTRACT

Prostate cancer is the second leading cause of cancer death in men. Prostate Specific Antigen (PSA) is the current indicator of prostate health, and needle core biopsy of the prostate is the standard of cancer diagnosis. However, PSA is not a specific indicator of cancer, and biopsy may miss actual tumor cells, leading to both false positive and false negative results, respectively. Therefore, better indicators of prostate cancer need to be identified.

Field effect is the term used to describe the existence of genetically altered, although histologically normal, cells that surround an area of frank cancer. Better understanding and characterization of this field should provide more sensitive means of detecting prostate cancer independent of histological biopsy findings that may miss the tumor. This study furthers field characterization by analyzing various types of genomic and epigenetic alterations, including gene promoter methylation, mRNA expression profiling, changes in telomeres, and genomic instability as reflected by random sites of allelic imbalance. Results demonstrate that this field is predictably altered in cancer.

TABLE OF CONTENTS

List of Figures

List of Tables

Chapter 1

Introduction

Background

Prostate cancer is the most common cancer related death in men after lung cancer in the United States. It is projected by the American Cancer Association that approximately 186,320 new cases will be diagnosed in 2008, with approximately 28,660 deaths-about 1 death every 16 minutes. That means there is a one in six chance of a man developing prostate cancer over his lifetime. Additionally, prostate abnormalities related to hyperplastic disorders, such as benign prostatic hyperplasia (BPH), prostatic inflammatory neoplasia (PIN), and adenocarcinoma, significantly impact quality of life due to nocturia, urinary retention, and sexual dysfunction (*1*). While the mechanisms of initiation and progression of these pathologies are not yet well understood, there is a strong correlation between advancing age and increasing incidence, with 80% of new prostate cancer diagnoses occurring in men 65 years and older (*1*).

In order to better understand prostate cancer, it is necessary to know about the normal prostate. The prostate is a small, walnut sized organ, approximately 20 grams, located retroperitoneally and encircling the neck of the bladder and the urethra. In the embryo, the prostate has fives lobes, but these lobes are indistinguishable in the adult prostate. The adult prostate is divided into four anatomical regions, specifically the peripheral, central, transitional, and periurethral regions (Figure 1). Most hyperplasias

arise from the transitional and periurethral regions, while most (70%) carcinomas arise

from the peripheral region.
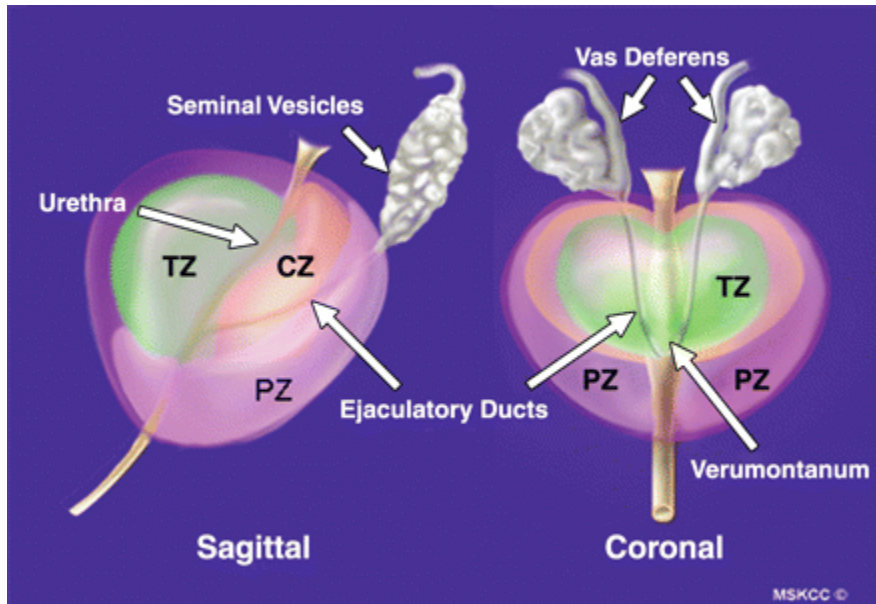
Figure 1. Zonal schematic of the prostate gland. Representation of the normal prostate
and its regions/zones. TZ=transitional zone, CZ=central zone, PZ= peripheral zone.
(http://www.ajronline.org/cgi/content-nw/full/188/5/1373)

The most common pathology of the prostate is benign nodular enlargement,

frequently referred to as benign prostatic hyperplasia (BPH). Nodules are commonly

located in the periurethral tissue, are visually distinct, and their growth has been linked to

androgen stimulation. These benign growths begin in the epithelial tissue and move into

the stromal compartment, resulting in prostates weighing anywhere from 60-200 grams or

more. The second most common pathology of the prostate is adenocarcinoma, and is

epithelial in origin. However, 90% of these tumors do not cause clinical symptoms, but

rather are discovered incidentally (*2*). The incidence of clinically significant prostate

cancer is very low in men of Asian ancestry, while it is most frequently found in African Americans, although Asians do have the same rate of latent disease as Caucasians (*3*). Prostatitis is the third most common pathology, and falls into three categories, acute bacterial, chronic bacterial, and chronic abacterial prostatitis. Prostatitis and BPH are significant in the prostate cancer story because BPH is often found in association with prostate cancer, both can cause symptoms similar to cancer, and both can cause prostate specific antigen (PSA) levels to rise.

PSA is the current early indicator of prostate cancer detection. It is a serine protease meant to cleave and liquefy seminal fluid coagulum formed in the ejaculate. In the instance of BPH, prostatitis, and carcinoma, PSA levels in the blood become elevated. However, this is the downfall of the PSA assay as well, as PSA cannot distinguish between BPH and carcinoma, nor can it provide information regarding the severity of disease. To further complicate the picture, some men simply produce higher levels of PSA normally (*4*). 25-30% of BPH cases and 80% of carcinoma cases have a PSA above 4 ng/ml, a level often considered to be the limit of normal PSA range (*5*). Of more concern, 20-40% of organ confined cases of prostate cancer have PSA levels in the normal range of 4 ng/ml or less (*4, 5*). The other routine test to detect prostate abnormalities is the digital rectal exam (DRE), where the prostate is palpated by a physician. However this test also has drawbacks, as it depends on the clinical experience of the practitioner to differentiate abnormalities and it can only detect a fairly large abnormality. Because PSA and DRE tests are not definitively diagnostic, histology is used to diagnose cancer of the prostate. This is done by taking 6-12 needle core biopsies of the prostate, usually guided by ultrasound. It is possible that any tumor cells present

may be missed in the standard six or twelve core biopsy, or multiple biopsies may be done over time because of the elevated PSA, often to the detriment of the patient (*6*). Most frightening to cancer patients following treatment with prostatectomy, PSA levels may actually rise temporarily, causing great distress (*7*). Yet, to date, no better biomarker has been found, either for detecting prostate cancer or for its prognosis (*4*). Taken together, these problems cause significant distress to patients and their families (*8, 9*).
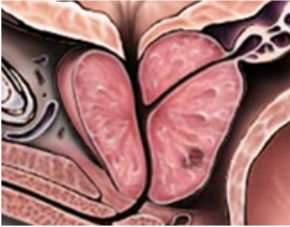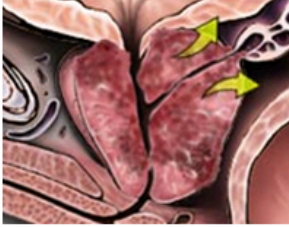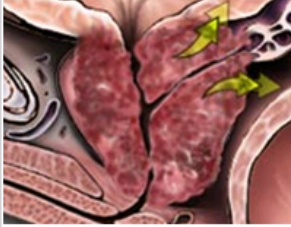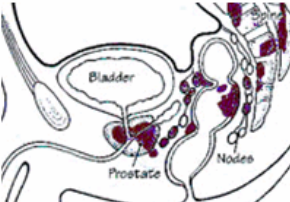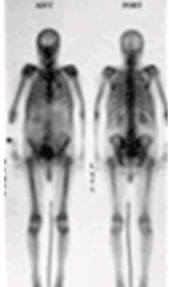
The prostate is a gland, and as such is comprised of glandular tissue, epithelial cells supported by basement membrane and surrounded by stroma. The general appearance is regular and orderly with small nuclei. Cancerous tissue frequently lacks basal cells and a basement membrane. The nuclei are large and vacuolated and cells contain large nucleoli. The general appearance is disorganized and irregular. The amount of dedifferentiation evident in a biopsy is prognostic, and in order to describe the abnormal histology, the Gleason Scale was developed. The scale runs from 1 to 5, where 1 is the most differentiated tumor and 5 is very dedifferentiated (Figure 2). The Gleason Score is a sum of the Gleason rating of the most prevalent (>50%) abnormal histology present, and the second score represents less than 50% but more than 5% of the observed cancer. Another possible histological finding is prostatic intraepithelial neoplasia (PIN). This is a transitional state between normal and cancerous histology, and is considered to be preneoplastic. PIN is characterized by multiple foci of glands with intra-acinar proliferation of cells with nuclear anaplasia. However there is no invasion and the basal layer and basement membrane are intact.
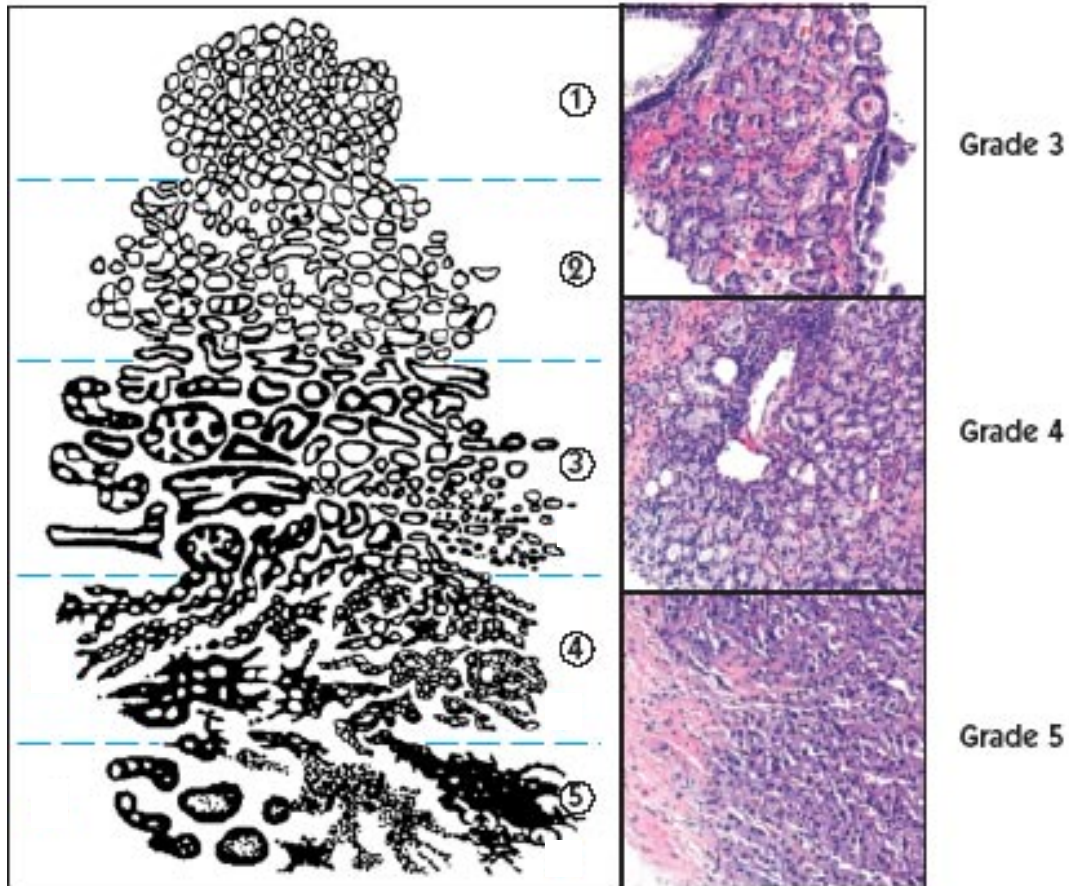
Figure 2. Gleason grading system diagram. The cartoon on the left is the pathological guide to grades 1-5. On the right are H&E stained slides that show examples of grades 3-5. (http://www.prostatecancer.org/education/staging/img/Dowd_GleasonScoreFig1.jpg)

If cancer is detected in a needle core, several treatment options are available to the patient, including radiotherapy and hormonal therapies. The definitive treatment for prostate carcinoma is surgical, a radical prostatectomy. All of these therapies include significant risk to the patient, the more significant risks ranging from loss of sexual function to incontinence to death. Prostatectomy can provide additional prognostic information, including perineural invasion, lymph node involvement, seminal vesicle involvement, and how much of the prostate is involved. Based on these additional

findings, patients can be staged by the TNM staging system (Figure 3). This system takes into account how much of the gland is involved, if lymph nodes are involved, and if there is disseminated disease. Complications of untreated disease can seriously affect quality of life and include metastasis and increased risk of morbidity. Advanced disease frequently spreads to the axial skeleton, specifically the spine, and can cause both osteolytic and osteoblastic bone lesions, although it should be noted that osteoblastic metastases are unique to prostate cancer and occur more frequently.

Figure 3. Staging of prostate cancers. Representative rubric of prostate tumor staging based on size (T), nodal involvement (N), and localization (M). (http://edoc.hu-berlin.de/dissertationen/kaiser-simone-2004-06-10/HTML/chapter1.html)

Another unique aspect of prostate cancer is its usually slowly progressing nature. Autopsy studies of elderly men frequently reveal the presence of undiagnosed prostate cancer that never manifested itself clinically (*1*). Often a man with a diagnosis of prostate cancer will die from another cause. While the American Cancer Society states 1 in 6 men will be diagnosed with this cancer, they also note that only 1 in 35 men will die from this disease. Because of this, men may choose not to treat this cancer, and rather engage in 'watchful waiting.' This is a valid treatment modality for many men, yet it is not appropriate for all men. PSA levels do not determine which men may benefit from watchful waiting. Finding a prognostic marker would be beneficial in this respect, significantly reducing the risk of mortality due to cancer and/or surgery and the risks associated with prostatectomy, including impotence, incontinence, and death.

Carcinogenesis is currently accepted to be a multi-step process. Genetic and epigenetic changes occur affecting the cell's regulatory mechanisms, leading to the loss of normal regulation and increased proliferation when these changes convey properties that enhance cell survival (*10, 11*). Importantly, it has been observed that (i) these changes are stable at the DNA level, allowing for genetic-based detection, and (ii) the microenvironment is critical to cancer development and behavior (*12*). As these mechanisms are clarified, new targets for detection, treatment, and prevention will lend themselves to development.

Genomic instability is one hallmark of cancer progression. One type of genomic instability, described as chromosomal instability, was first characterized by Lengauer and colleagues (*13*). A tumor cell population with chromosomal instability indicates high

clonal heterogeneity (*14*). DeWever and Mareel (*15*) have proposed a model of intimate interaction between tumor and stroma to explain the observed DNA changes, which also explains a phenomena referred to as the observed field effect well. The term "field effect refers" to the observation of genomic changes not only within tumor cells, but the surrounding tissues as well, despite the fact that these tissues appear histologically normal. Changes may occur along one of two pathways. In the efferent pathway, the tumor cell exerts an effect on the surrounding stroma, causing it to secrete products such as PDGF and TGFβ. The stroma is now termed reactive stroma as it is altered or transdifferentiated. The afferent pathway is one by which this reactive stroma then affects the tumor cells, releasing proinvasive signals that enhance motility and invasion properties of cells and also reduces apoptosis. Reactive stroma also plays a role in cancer pain and directing cancer cells to perineural invasion and dissemination (*12*).

This scenario requires highly specific interactions under specific conditions, namely the environment must be receptive to some initial stimulus at the right time and location. Experiments have demonstrated that tumors will grow when cancer cells are seeded into reactive stroma, but not when seeded into normal stroma (*12*). *This suggests that the microenvironment must be created first, potentially allowing for early detection, provided we know what genetic or epigenetic profile to look for.* These alterations are not terminal events in cancer progression, but rather are ubiquitous within a field of genomically unstable cells during cancer progression. Because these events may be found outside the focus of tumor cells or even before tumor cells are present, they are more likely to be found in the tissue of a needle core biopsy. mRNA transcript levels, gene promoter methylation, telomere alteration, and microsatellite instability are among the

possible alterations likely to be present early in the development of prostate cancer, and therefore may have significance in early diagnosis (*16-21*).

One such example of epigenetic profile alteration is GSTP1 methylation, observed in PIA, PIN and prostate cancer, but not BPH, suggesting that some event initiates instability, providing the driving force for prostate cancer progression (*18-20, 22*). Another example of genomic instability can be seen in telomeres, a naturally inherent barrier to the development of cancer. Telomeres are specialized protein-nucleic acid structures that protect and stabilize the ends of eukaryotic chromosomes (*23, 24*). When telomere lengths are reduced beyond a critical set point, they become prone to chromosomal fusion and breakage, normally causing activation of the p53 pathway in healthy somatic cells, which will then progress through senescence and apoptosis (*25-30*). These mechanisms are frequently inactivated in cancer cells, for example through p53 and Rb mutations or hypermethylation silencing of GSTP1 or P504S (*31-33*). Accordingly, telomere shortening in cancer cells is a cause of unchecked genomic instability, including dicentric chromosome formation, chromosome translocation, aneuploidy and loss of heterozigosity and, thus, a source of phenotypic variability (*30, 34-36*). In retrospective studies, our laboratory has shown that telomere content (TC), a surrogate for telomere length, predicts clinical outcome in prostate cancer (Figure 4) (*37*). Similarly, TC in tumor adjacent histologically normal (TAHN) tissue, taken 1 cm distant from the tumor margin, also correlated well with clinical outcome in prostate cancer (*38*). While the current method of measuring TC is very effective, it does not lend itself well to direct application in the clinical setting for various reasons (*39*). Therefore, despite TC providing a sensitive predictor of disease-free survival in men with prostate cancer, an

alternative marker and/or method for use with samples containing small numbers of cells, such as needle core biopsies, using common techniques and equipment, such as PCR, is desirable.
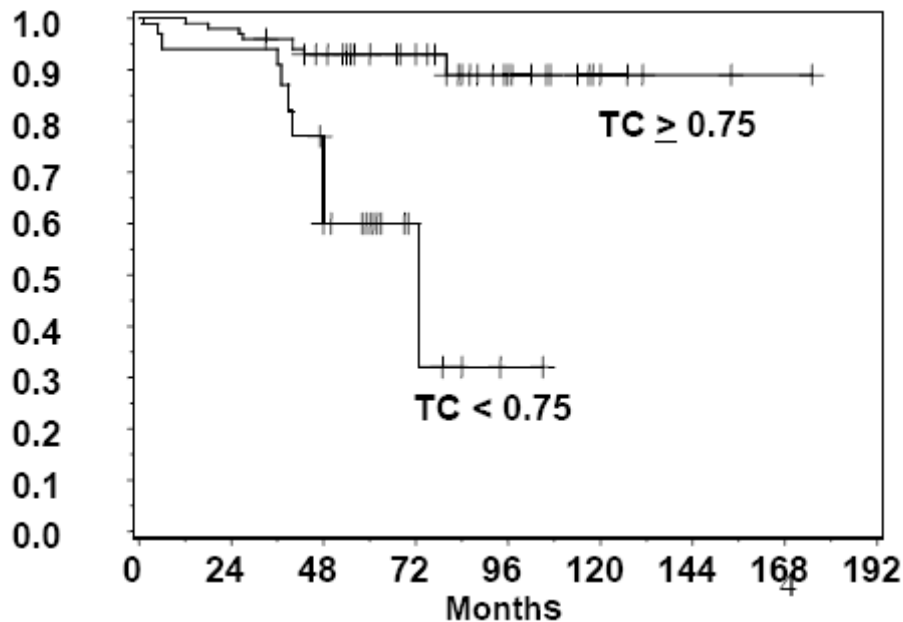
Figure 4. Covariate-adjusted recurrence free survival by telomere DNA content in prostate tumors. The cohort was divided into two groups, based on the specified values of telomere DNA content (TC). The first group contained samples with TC >0.75 (N=49). The second group contained samples with TC <0.75 (N=28). The prostate cancer-free survival interval, in months, is shown on the x-axis and the recurrence-free fraction is shown on the y-axis. Censored events are indicated with ticks. (*38*)

Given that many types of genetic and epigenetic changes have been documented, it seems logical that these changes should be reflected in the messenger RNA (mRNA) produced by a cell, and that these changes should be quantifiable. And indeed, this can be done using microarray technology, through the labeling of cDNA generated from mRNA

and competitive hybridization to specific probes (*40*). This technique is becoming common place in laboratories and is establishing unique cancer profiles. The hope in using this technique is to identify a unique 'signature' for a given tumor type for use as a diagnostic tool (*41-44*). Additionally, this method can also be used to identify genes of interest, genes worth further evaluation for methylation or recombination, due to the specificity of the probes, and the presence of several probes for each gene, revealing splice variants. While microarray analysis requires a minimum amount of mRNA, the rapid turn around time and wealth of data generated make this a valuable tool for rapid assessment of the transcriptome and focusing of studies.

Chapter 2

Rationale and Hypothesis

Rationale

Using the method for measuring telomere DNA content (TC) developed in our

laboratory (*39*), we previously reported an association between TC and overall survival

and biochemical recurrence (rising PSA) in a small, case-control study of 18 men with

prostate cancer (*37*). These findings have been confirmed by measuring TC in archival

prostate tissue obtained from a cohort of 77 men treated with prostatectomy between

1982 and 1995 (*38*). Most tumors were Gleason Grade of 6-7 and had not spread to the

pelvic nodes. The median age at diagnosis was 67 years. The cohort was divided into

three groups of approximately equal size based on TC and a Cox proportional hazards

model of time until recurrence or death from prostate cancer was developed (Table 1).

The variables included tumor TC, age at diagnosis, pelvic node involvement and Gleason

sum score. There was no increased risk of recurrence associated with TC values of 0.75 –

1.49. However, TC values <0.75 conferred a relative hazard of 5.02 (p=0.0132). By

comparison, the relative hazard conferred by pelvic node involvement was 6.50

(p=0.0002) and Gleason sum scores of 7, and 8 or more, were 4.54 and 5.96, respectively

(p=0.0292 and p=0.0210, respectively). Recurrence-free survival for men with TC of

>0.75, and <75, is shown in Figure 4. TC values of <0.75 predicted prostate cancer

recurrence with a specificity of 0.90 (95% CI of 0.78-0.97). Wilcoxon/Kruskal Wallis

Rank Sums Analysis indicated a statistically significant lower median TC in men whose

Table 1: Recurrence-free survival by telomere DNA content (TC) in a cohort of 77 cancer patients, adjusted for age, Gleason score, and pelvic node involvement. [1]Relative hazard (RH) and 95% confidence intervals (CI) from Cox proportional hazards model of time until recurrence or death from prostate cancer. [2]Telomere DNA content (TC).

Variable	Level	[1]RH (95% CI)	p-Value
Age	Slope (per 10 years)	0.28 (0.10, 0.77)	0.01
Gleason score	2 - 6	1.00	
	7	4.54 (1.17, 17.72)	0.03
	8 – 9	5.96 (1.31, 27.17)	0.02
Pelvic Nodes	Negative	1.00	
	Positive	6.50 (2.41, 17.51)	<0.001
[2]TC N=25	$\geq$ 1.50	1.00	
N=24	0.75 – 1.49	1.00 (0.22, 4.65)	0.99
N=28	< 0.75	5.02 (1.40, 17.96)	0.01

cancer recurred within 6 years (p=0.012) than in men who remained free of disease during the same time (Figure 5, left panel).
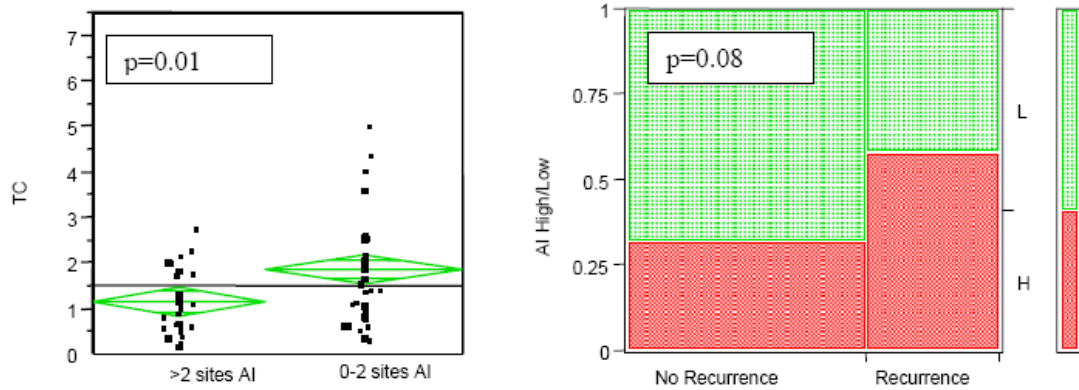
Figure 5: Association between telomere DNA content, allelic imbalance and 72-month recurrence-free survival in prostate tumors. Left panel: Non parametric Wilcoxon/Kruskal-Wallis Rank Sum analysis of the relationship between telomere DNA content (TC) and allelic imbalance (AI) in 64 prostate tumors. TC was measured as described in the Chapter 5. AI was based on the ratios of paired alleles' signal intensities. The mean ratio in 318 heterozygous loci in buccal cells from 28 healthy individuals was 1.14 (SD 0.18). Thus, 99% of loci from normal cells would be expected to have allelic ratios less than 1.59 (i.e., mean +2.5 SD). Therefore, a site of allelic imbalance was defined when the ratio of the paired alleles' signal intensities was 1.6, or greater. The line across each diamond represents the group mean. The height of each diamond represents the 95% confidence interval for each group, and the diamond width represents the group sample size. Right panel: Data was obtained from 53 men without prostate cancer recurrence within 72 months after prostatectomy and men with documented distant metastasis, biochemical recurrence (rising PSA) or death as a consequence of prostate cancer within 72 months after prostatectomy. Data was grouped by recurrence status and high or low allelic imbalance. High AI was defined three or more sites, low as 0-2 sites.

Based on these results, we reasoned that other direct quantitative measurement of genomic instability would have similar prognostic value. To evaluate this possibility, we

investigated the relationships between AI and TC in prostate cancer tissues and the

relationship between AI in prostate cancer tissues and 6-year disease-free survival

(Figure 5). Allelic imbalance was evaluated using a PCR based assay similar to that

described previously (*17, 45, 46*). The AmpFlSTR® kit (Applied Biosystems, Foster

City, CA) contains reagents that amplify 16 different short tandem repeat (i.e.

microsatellite) loci within a single multiplex reaction. TC was determined using the slot

blot titration assay developed in our laboratory (*39, 47*). Samples were divided into two

groups, high and low, based on the extent of AI. "High" was defined as three or more

sites of AI, as determined by dividing the smaller into the larger peak height with 1.61

and above considered imbalanced, and "low" as fewer than three sites of AI. Analyzing

the data by Wilcoxon/Kruskal-Wallis Rank Sum Tests, there was an inverse correlation

between TC and AI (p=0.01, N=64), When the sample was divided based on recurrence

of prostate cancer within 6 years of prostatectomy, there was a near significant

relationship between the group of men whose cancer recurred and the group with three or

more sites of AI (p=0.08, N=53).

Hypothesis

   We have previously shown that the extent of genomic instability, measured by

either AI or TC is similar in tumor and TAHN tissue (*17, 38, 48*). We propose that the

distribution of these molecular alterations reflects a "field" of genetically altered cells,

within which resides a subpopulation in which tumor progression has also resulted in

histological changes. We further propose that it is these genetic alterations, not the

histological characteristics of the cells that have the greater diagnostic and prognostic

significance. It is with this in mind that we hypothesize that we will observe similar distributions of markers of hypermethylation patterning, and gene expression profiles in prostate tumors and TAHN tissues, which will differ from those patterns observed in truly normal prostate tissues from men without cancer. We further hypothesize that like TC and AI, some of these markers will differ between prostate tumors or TAHN tissues from men whose prostate cancer did and did not recur. This approach has the potential to define genes whose expression is essential for prostate cancer progression and markers that can be used for both diagnosis and prognosis that are independent of frank histological change. By doing so, more timely care and a reduction in the risk of undesirable side effects to the patient should occur through better identification of patients in need of treatment.

Specific Aims

To test the hypothesis of this study, several modalities will be employed. These include gene expression analysis using spotted microarrays and genomic and epigenomic changes measured by TC, AI and methylation status analysis. We and others have previously shown that the extent of genomic instability, measured by either AI or TC, is similar in tumor and TAHN tissue, and may be an independent marker of prognosis (*38, 49, 50*). These findings also support the field effect model. However, the field effect in prostate cancer is still being investigated because of the likely implications involving cancer. Avenues of investigation include gene expression analysis, which also ties into methylation status of gene promoters, and will be a part of the focus of this study. We will test this hypothesis by completing the following four aims.

• **Specific Aim #1:** *Compare methylation states of genes known to be associated with prostate cancer, such as GSTP1, APC, RARB2, and RassF1A, between tumor cells, patient matched TAHN tissue and normal prostate tissue from men without cancer.*

• **Specific Aim #2**: *Assess characteristic changes in gene expression with microarrays relevant to prognosis in prostate cancer, and determine if this profile extends to surrounding histologically normal cells.*

• **Specific Aim #3:** *Use the telomere content assay to detect and predict potential disease relapse in retrospective studies of prostate cancer cases with patient matched negative biopsy, positive biopsy, TAHN and tumor tissue samples.*

• **Specific Aim #4:** *Use the allelic imbalance assay to detect and predict potential disease relapse in retrospective studies of prostate cancer cases with patient matched negative biopsy, positive biopsy, TAHN and tumor tissue samples.*

Chapter 3

Methylation in Prostate Cancer

Specific Aim: Evaluate and compare methylation status of genes known to be associated with prostate cancer (GSTP1, Rarβ2, APC, and RassF1A) in cancerous and histologically normal prostate tissues to determine if epigenetic changes that may aid in the early detection of cancer exist in TAHN tissues.

      Introduction: It is commonly accepted that changes in gene expression, such as a down-regulation and/or mutation of p53 or increased expression of growth factor genes are ubiquitous in cancers (*32*). Increases or decreases of expression are often attributable to changes in the methylation state of CpG islands, GC-rich sequences found in the promoters of genes. CpG islands are normally unmethylated, with the exceptions of the inactive X chromosome, imprinted genes, tissue specific genes, and those that are developmentally regulated by methylation (*51*). It has been observed that tumors of specific tissues possess additional unique methylation patterns in specific genes (*4, 52, 53*) and may be predictive of outcome (*17-19, 33, 54-61*).Some of these changes have been observed regarding prostate cancer. Examples of genes frequently showing promoter methylation include GSTP1, APC, RassF1A, RARβ2, P504S, and CRBP1 (*18, 19, 31, 56, 58, 62-64*) However, most of these studies have focused on methylation of tumor cell promoters, and have not focused on field investigation. Based on previous studies demonstrating field effect within the laboratory, we predicted that promoter methylation would also demonstrate field effect and should, therefore, be characterized.

Hypermethylation is a useful assay for measuring genomic stability for several reasons. First, methylation status is a positive assay that provides a result with a "yes or no" answer relative to a known constant (*52, 65*). Second, the methylation pattern of a particular tumor provides information on which specific genes are being turned on or off, which can predict particular phenotypes. An example of this is GSTP1, whose expression is associated with drug resistance and increased mortality (*66*). After a thorough review of the available literature, we proposed to compare the hypermethylation status of GSTP1, Rarβ2, APC, and RassF1A, between tumor tissue and TAHN tissue, as these had previously been associated with prostate cancer (*52, 53, 67*). Based on previous studies with AI and TC, we predicted that the TAHN tissue will demonstrate a similar pattern as that found in the tumor. A future possibility is the detection of prostate cancer using methylation status of specific genes to detect cancer in other sample types, specifically TAHN tissues of core biopsies (*68, 69*). Using hypermethylation assays in this way could allow for earlier, more sensitive detection of prostate cancer and reduce the number of repeated biopsies, thus reducing risk to the patient.

Methylation-specific PCR (MSP) is a simple, efficient method of detecting methylation of specific genes. By using gene-specific primers, the methylation state of CpG islands can be detected from small amounts of sample DNA, including those derived from fresh frozen samples or micro-dissected samples (*65*). Because increased frequency of CpG sites indicates a possible area of methylation, detection is achieved by using two primers, one specific to the methylated allele (M), the other specific to the unmethylated allele (U), exploiting the sequence differences between alleles following bisulfite treatment. Primers are designed to generate products between 80-200bp in size.

This technique has been shown to be incredibly sensitive without loss of specificity under optimal conditions (*66, 68, 70*). Sample DNA is treated with sodium bisulfite, causing the conversion of unmethylated cytosine to uracil, without affecting methylated cytosines. Removal of bisulfite completes the preparation of the template DNA for PCR.

Materials and Methods

Prostate sample collection, preparation, and demographics: Thirteen matched prostate tumors and TAHN tissues excised at 1cm from the visible tumor margin, resulting in a total of 26 samples, were obtained from the University of New Mexico Hospital Pathology Laboratory in agreement with all University, State and Federal laws. Tissue samples were snap frozen in liquid nitrogen immediately after collection and stored at -70˚C. A portion of the frozen tissues (approximately 50-70 mg) was homogenized and DNA was isolated and resuspended in TE buffer (DNeasy Kit, Qiagen, Valencia, CA). The median age of the cohort was 58.5 years with a range was 50-71 years; all samples had Gleason scores of 3+3 or 3+4, and a Stage of T2 with the exception of two T3 cases; all samples were node negative (Table 2).

Eight prostate samples from cancer-free controls (sudden death cases) were obtained from the National Cancer Institute Cooperative Human Tissue Network (CHTN; Nashville, TN), stored at -70˚C, and subjected to DNA extraction. The median age of this set was 44.5 years, with a range of 0-79 years (Table 2). An additional fully methylated DNA positive control, CpGenome Universal Methylated DNA, was obtained from Millipore (Temecula, CA)

Cell Lines: Cell lines (LnCaP, DU146, C4-2b, and PC-3) were used to verify the performance of the assay (*i.e.* if the primers and sodium bisulfite treatment were functioning properly). These lines represent a range of prostate cancer and gene promoter methylation.

Treatment of DNA with Sodium Bisulfite: Following DNA extraction, DNA was treated with the commercially available sodium bisulfite-based kit CpGenome fast DNA modification kit (Millipore, Temecula, CA) to cause deamination of unmethylated cytosines in the CpG repeats.

Detection of Gene Methylation: Primers used here were previously published (*18, 55, 58*) (Table 3). Semi-quantitative methylation specific PCR (QMSP) utilized methylated DNA specific TaqMan probes to detect methylated samples was used to detect methylation of samples. In this technique, 1 uL of the sodium bisulfite treated DNA was combined with 10 uL of 2x TaqMan Universal PCR Kit (Applied Biosystems, Foster City, CA), 600 nmol of each primer, 200 nmol probe, and the remaining volume water for a total of 20 uL. The reactions were run on an ABI PRISM 7000 real time PCR machine with the following protocol: Initial denaturation at 95°C for 10 minutes followed by 50 cycles of 95°C for 15 seconds then 60°C for one minute (*18, 19, 56*). All samples

Table 2. Study cohort of methylation study.

Sample	Age	Grade	Stage
S04 175	64	3+3	T2 N0/II
S04 4063	57	3+3	T2/II
S04 4778	71	3+4	T3 N0/III
S04 8506	64	3+3	T2a N0/II
SUH-05-1070	60	3+4	T2a N0/II
SUH-05-1083	55	3+3	T2c/II
S05 1319	57	3+4	T2c N0/II
S05 1329	50	3+3	T2c N0/II
S05 2452	53	3+3	T2c N0/II
S05 3237	53	3+4	T2c/II
S05 3494	60	2+3	T2a/II
S05 3855	65	3+4	T2c/II
S05 8524	52	3+4	T2c N0/II
P7550	Infant	Normal	
P7551	Infant	Normal	
38166	79	Normal	
39196	43	Normal	
39306	55	Normal	
38975	46	Normal	
Z4061227E	43	Normal	
Z4070022A	26	Normal	

Table 3. **Primers and probes used for Q-MSP**. The left column indicates the primer/probe designation, the right column indicates the sequence of the oligonucleotide and fluorescent labels (for probes).

Designation	Oligonucleotide Sequence
Rar-β2 Forward	5'-CGA GAA CGC GAG CGA TTC-3'
Rar-β2 Reverse	5'-CAA ACT TAC TCG ACC AAT CCA ACC-3'
Rar-β2 Probe	5'-6-FAM-TCG GAA CGT ATT CGG AAG GTT TTT TGT AAG TAT TT-6-TAMSp-3'
β-actin Forward	5'-TGG TGA TGG AGG AGG TTT AGT AAG-3'
β-actin Reverse	5'-ACC CAA TAA AAC CTA CTC CTC CCT TAA-3'
β-actin Probe	5'-6-FAM-ACC ACC ACC CAA CAC ACA ATA ACA AAC ACA-6-TAMSp-3'
GSTP-1 Forward	5'-AGT TGC CGC GCG ATT-3'
GSTP-1 Reverse	5'-GCC CCA ATA CTA AAT CAC GAC G-3'
GSTP-1 Probe	5'-6-FAM-CGG TCG ACG TTC GGG GTG TAG CG-6-TAMSp-3'
RassF1A Forward	5'-GCG TTG AAG TCG GGG TTC-3'
RassF1A Reverse	5'-CCC GTA CTT CGC TAA CTT TAA ACG-3'
RassF1A Probe	5'-6-FAM-ACA AAC GCG AAC CGA ACG AAA CCA-6-TAMSp-3'
APC Forward	5'-GAA CCA AAA CGC TCC CCA T-3'
APC Reverse	5'-TTA TAT GTC GGT TAC GTG CGT TTA TAT-3'
APC Probe	5'-6-FAM-CCC GTC GAA AAC CCG CCG ATT A-6-TAMSp-3'

were run in quadruplicate, and a promoter specific to unmethylated β-actin was used as the internal control. To determine levels of methylation, the delta Ct of a sample was divided by the delta Ct of β-actin and then multiplied by 100 to give a representative methylation level. Controls included a no template control and a fully methylated DNA control (CpGenome™ Universal Methylated DNA, Millipore, Temecula, CA). In order for the data to be considered acceptable, there needed to be at least three data points reflecting the threshold of detection of the probe, which were then averaged and used in the calculation of relative methylation.

Results:

In all instances, the promoters of the genes of interest, in addition to the β-actin control, were unmethylated in DNA from normal tissues (Figure 6).

In contrast, promoter methylation for some, but not all genes was detected in Tumor and TAHN samples (Figure 7). While the GSTP1 assay successfully identified methylation in cell lines, it did not detect methylation in patient samples, contrary to previously published studies of GSTP1 methylation in cancer. Rar-β2 was methylated in one instance of Tumor DNA. APC was methylated in four tumor samples, but none of the TAHN samples (Figure 8). RassF1A displayed frequent promoter methylation in tumor samples, and was in four samples of the matched TAHN tissues (Figure 9). See Table 4 for a summary of results.
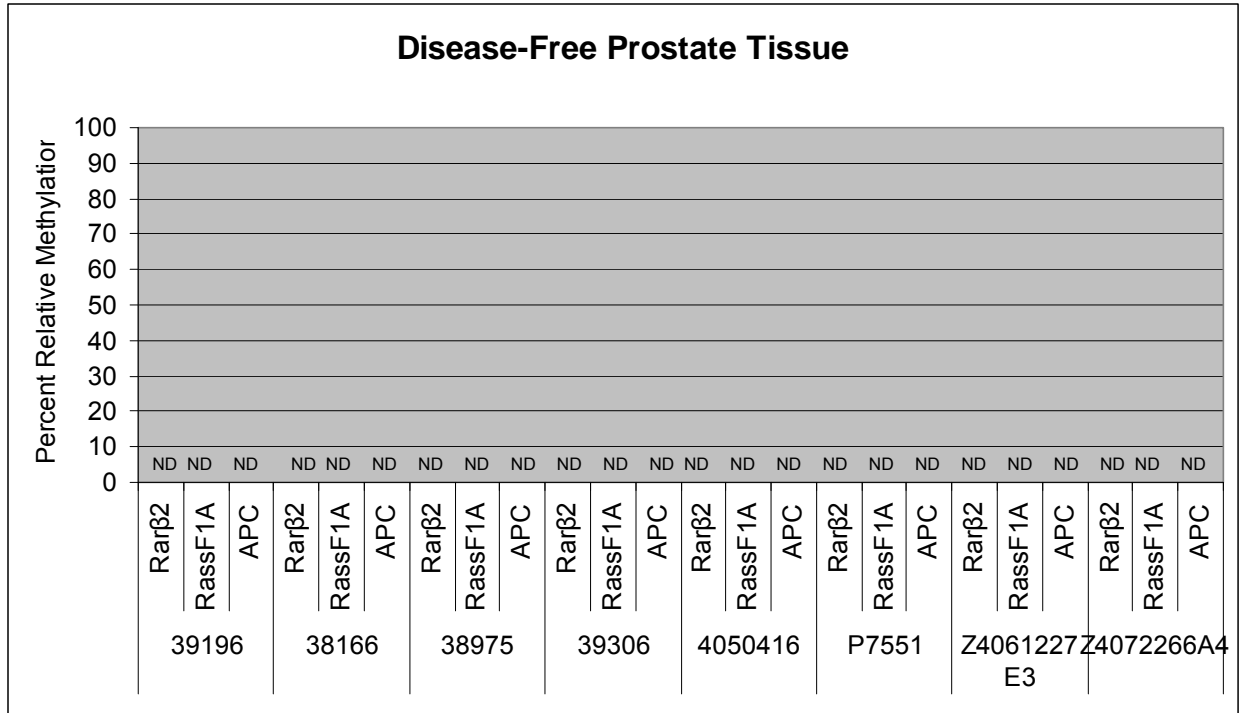
Figure 6. DNA from disease-free prostate tissues. Included are a post-mortem DNA sample of prostate tissue from an infant (P7551), and six post-mortem DNA samples from adults shown to be free of prostate disease (39306, 39196, 38166, 28975, 29206, Z4061227E3, Z4072255A4). All samples were analyzed for methylation with the promoters for Rar-B2, APC, Rass F1A, and GSTP-1. In all cases all gene promoters were found to be unmethylated. B-actin was the internal reference control used to normalize assay results (not shown). ND=not detected.
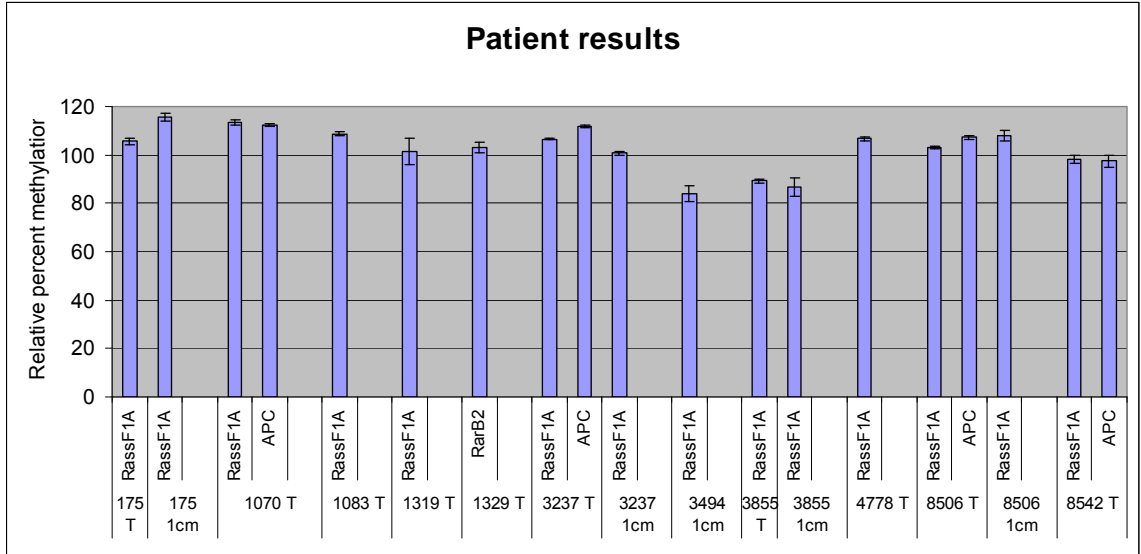
Figure 7. Patient sample methylation status. Results to date of tumor and matched NHN tissue. The X axis denotes the patient sample, tissue type (T=tumor, 1cm=NHN). Shown on the Y axis is the relative percent methylation. To determine relative percent methylation, the delta Ct of the sample is divided by the delta Ct of unmethylated β-actin and then multiplied by 100.
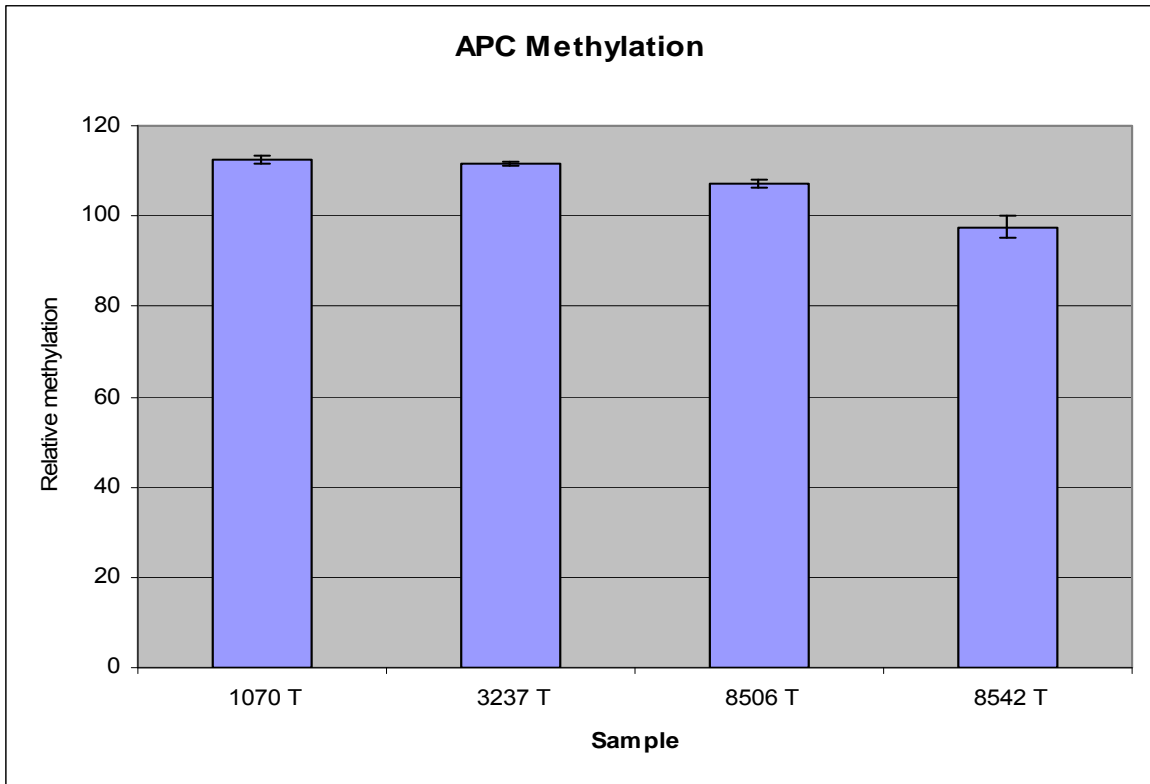
Figure 8. Methylation of the APC promoter. APC was only found to be methylated in the tumor tissue of four patients in the set of thirteen patients analyzed. The X axis denotes the patient sample, tissue type (T=tumor, 1cm=NHN). Shown on the Y axis is the relative percent methylation. To determine relative percent methylation, the delta Ct of the sample is divided by the delta Ct of unmethylated β-actin and then multiplied by 100.
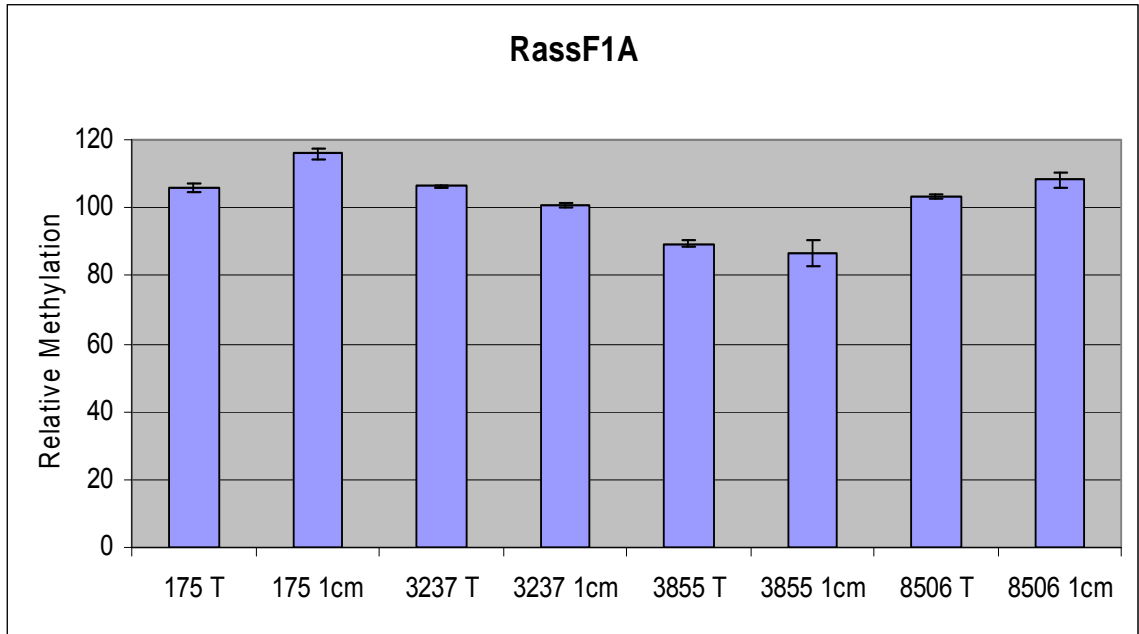
Figure 9. Methylation of RassF1A in matched patient samples. The X axis denotes the patient sample, tissue type (T=tumor, 1cm=NHN). Shown on the Y axis is the relative percent methylation. To determine relative percent methylation, the delta Ct of the sample is divided by the delta Ct of unmethylated β-actin and then multiplied by 100. RassF1A was found to be methylated in ten patient samples; shown here are the four matched patient samples of tumor and NHN tissue found to be methylated.

Table 4. Summary of methylation results.

Sample set	Gene	Positive for methylation
Tumor	RarB2	1/13
n=13	RassF1a	9/13
	APC	4/13
1cm	RarB2	0/13
n=13	RassF1a	5/13
	APC	0/13
Normal	RarB2	0/8
N=8	RassF1a	0/8
	APC	0/8

Discussion:

While global de-methylation is associated with the cancer genome, it is well known that methylation silencing of individual genes is also common. GSTP1 methylation is a well established phenomenon in cancer cells. However, while several studies have evaluated many genes, including GSTP1, RassF1A, Rar-β2, and APC, these studies have been plagued by a lack of proper controls, in that studies need to include truly normal, disease-free tissue, not tumor adjacent tissues, for establishing a base line level of methylation. This is particularly important in methylation studies where variable levels of methylation have been observed not only in tumors but in other pathologies of the prostate as well. This study endeavored to demonstrate why this is important by showing the existence of a field of altered cells in the tissues surrounding the tumor. As illustrated by the Rar-β2 results, this field of alteration does exist around a tumor, but as evidenced by the APC results, the extent of alterations in adjacent tissue is variable. This is particularly important as the methylation pattern of particular genes appear to differ in tumor and TAHN tissues. While this study is not definitive, it does agree with published data, particularly the Mehrotra study (*20*), and indicates that further investigation of these genes is warranted. Further investigation may lead to a new diagnostic tool to detect prostate cancer with out the presence of tumor cells in a biopsy, as well as differentiate between cancer and other pathologies such as PIN and BPH.

Chapter 4

Microarray and Prostate Cancer Field Effect

Specific Aim: Assess characteristic changes in gene expression by spotted microarray analysis of tumor and TAHN tissues to investigate the field effect.

Introduction: The terms "field cancerization" or "field effect" were first introduced in tumors of the head and neck to describe the occurrence of genetic alterations in histologically normal tissues adjacent to tumors (*71-74*). Such alterations outside of the histologically visible tumor margins could result from pre-existing fields of genetically compromised cells in which the tumor develops. Alternatively, the tumor could influence the surrounding tissue, or it may reflect a combination of these two scenarios. While the underlying mechanisms of field cancerization remain unclear, its occurrence has been described in several epithelial cell derived tumors, including but not limited to lung, esophageal, colorectal, breast, and skin cancers (*71, 74, 75*). In contrast, relatively little is known about field cancerization in prostate cancer, perhaps due to its previously reported multifocal nature (*75, 76*). In addition, prostate cancer is often present in the setting of other benign prostatic conditions, most frequently benign prostatic hyperplasia (BPH), which could influence adjacent cells and thus affect the characterization of field cancerized tissue. Finally, due to the relatively small size of the human prostate, the entire organ may be affected, either genetically or biochemically, excluding the existence of matched, truly normal, *i.e.* entirely unaffected tissue from the same patient.

Field cancerization is of clinical importance (*75*). In prostate cancer, markers of field cancerization may be important for confirming or detecting disease in biopsies after abnormal prostate specific antigen (PSA) and/or digital rectal examination (DRE), the current standard of care for detecting prostate cancer. PSA screening has led to earlier detection and an overall decrease in prostate cancer specific mortality, emphasizing the importance of prostate biopsies (*77, 78*). However, biopsy tissue represents a very small portion of the prostate and consists primarily of tumor adjacent histologically normal (TAHN) tissue. In spite of ultrasound guidance, it is easy to miss a small focal malignancy. The current accuracy of prostate cancer detection/confirmation by biopsy is approximately 25% with the rest representing false negative diagnoses (*79, 80*). In the presence of an abnormal PSA and/or DRE, this represents a dilemma for the patient and his physician. Therefore, biomarkers that are indicative of disease, yet independent of histology, i.e. present in field cancerized TAHN tissue, could greatly increase the accuracy of early prostate cancer detection in biopsies (*75*).

Our laboratory has previously investigated the nature of field cancerization in both prostate and breast cancers using markers of genomic instability, including telomere DNA content (TC), an established surrogate measure of telomere length, and the extent of allelic imbalance (AI) (*17, 38*). These studies have shown telomere alterations and the presence of AI in both tumor and TAHN tissues. In particular, alterations in TC seen in prostate tumors were frequently mimicked in the matched TAHN tissues, indicating prostatic field cancerization (*38*). Based on these observations, we hypothesized that the molecular changes would not be limited to genomic instability, but may include consistent alterations in gene expression. To test this hypothesis, we conducted a proof-

of-principle study utilizing microarray expression analysis of cancerous and TAHN prostatic tissues isolated at 1cm from the visible tumor margin. We report here the identification of consistently altered gene expression in TAHN tissues indicative of field cancerization in prostate cancer.

Materials and Methods

      Prostate sample collection, preparation, and demographics. Twelve matched prostate tumors and TAHN tissues excised at 1cm from the visible tumor margin (approximately 150 mg each), resulting in a total of 24 samples, were obtained from the University of New Mexico Hospital Pathology Laboratory in agreement with all University, State and Federal laws. Tissue samples were snap frozen in liquid nitrogen immediately after collection and stored at -70˚C. A portion of the frozen tissues (approximately 50-70 mg) was homogenized and RNA was isolated and resuspended in RNase-free water (Qiashredder and RNeasy Kits Qiagen, Valencia, CA). The median age of the cohort was 57 years with a range was 51-71 years; all samples had Gleason scores of 3+3 or 3+4, and a Stage of T2 with the exception of two T3 cases; all samples were node negative (Table 5).

      Samples were randomized into 2 groups, the microarray set (MA set, Table 1) and the validation set (VA set, Table 5). Each group consisted of 6 patient matched tumor and TAHN samples; the MA samples were those designated 1-6, while the VA set were the samples designated 7-12 in Table 5. Three matched sets of tissue (approximately 50-70 mg per sample) from both the MA and VA sets were formalin fixed and paraffin embedded for sectioning and hematoxylin & eosin (H&E) staining for independent

Table 5. Description of prostate samples used in the microarray study. The cohort

consisted of (i) 12 tumor and matched tumor adjacent histologically normal (TAHN)

human tissues collected at the University of New Mexico Health Sciences Center and (ii)

6 normal, cancer-free prostates obtained from the Cooperative Human Tissue Network.

Sample	Patient's Age	Gleason Score[1]	TNM Stage[1]
Tumor/TAHN			
1	58	3+3	T3/III
2	57	3+3	T2/II
3	71	3+4	T3 N0/III
4	64	3+3	T2a N0/II
5	53	3+3	T2c N0/II
6	57	3+4	T2c N0/II
7	51	3+4	T2c/II
8	60	3+4	T2a N0/II
9	50	3+3	T2c N0/II
10	55	3+3	T2c/II
11	64	3+3	T2 N0/II
12	53	3+4	T2c/II
Normal			
13	46	na[2]	na
14	55	na	na
15	43	na	na
16	79	na	na
17	26	na	na
18	43	na	na

[1] Tumor Nodes Metastasis (TNM) stage was assigned using criteria published by the

American Joint Committee on Cancer (http://www.cancerstaging.org/index.html).

Gleason scores and Stages were determined from the prostatectomy samples.

[2] Not applicable.

pathological review (Figure 10). For the six cases chosen for microarray analysis, a total of 1μg of the isolated RNA was pooled to generate the MA set, while the remaining RNAs and RNAs from six additional cases (independent VA set) were stored separately.
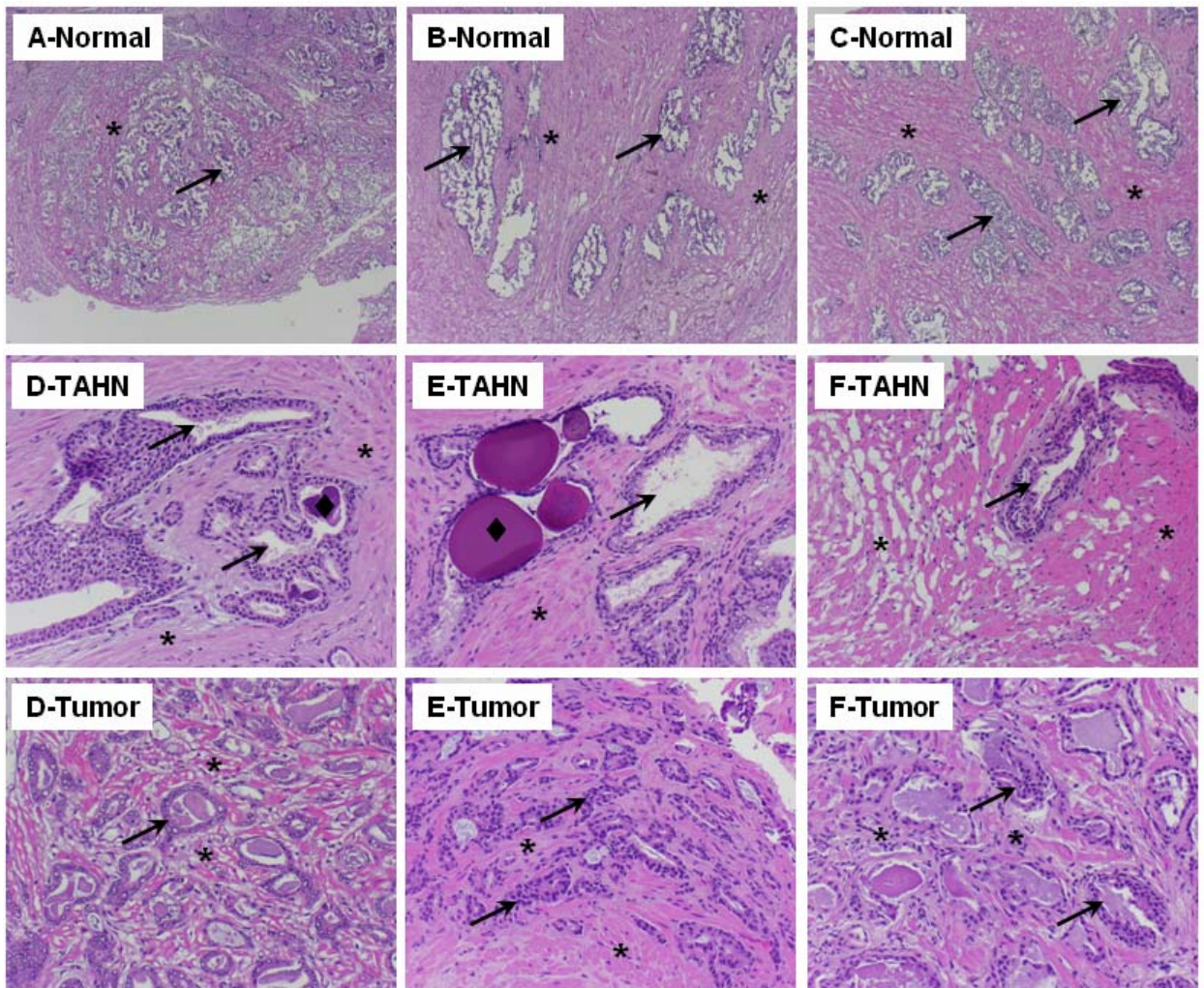
Figure 10. H&E staining of representative prostate tissues. H&E staining of 3 cancer-free normal prostate tissues (A-C) and 3 representative cases of tumor and tumor adjacent histologically normal (TAHN) tissues (D-F; cases 5, 6, and 8 in Table 1). A-C are at 40x magnification; D-E are at 200x magnification; arrows and asterisks denote glandular (ductal epithelial) and stromal areas, respectively; diamonds in D-TAHN and E-TAHN denote *corpora amylacea* (sedimented sulfated glycosaminoglycans) often seen in normal prostatic tissues (*81*).

Six prostate samples from cancer-free controls (sudden death cases) were obtained from the National Cancer Institute Cooperative Human Tissue Network (CHTN; Nashville, TN), stored at -70˚C, and subjected to RNA extraction and histological review. The latter confirmed these samples to be cancer-free and also free of BPH (Figure 10). The median age of this set was 44.5 years, with a range of 26-79 years (Table 8).

Microarray expression analysis. RNA integrity was analyzed using the Agilent Bioanalyzer 2100 (Agilent, Foster City, CA). RNAs from six matched tumor and TAHN tissues were selected to be prepared for microarray analysis based on RNA quality and quantity (the MA set). RNA from the selected samples was combined in equal parts to a total of 1µg to generate the tumor and TAHN pools for the MA set. Control RNA for microarray analysis was obtained from Ambion (Austin, TX). This consisted of RNA pooled from 9 Caucasian donors without prostate cancer (sudden death cases), and a median age of 70 years (range of 45-79 years).

RNA was reverse transcribed into complementary DNA (cDNA) using the Retroscript™ RT Kit (Ambion, Austin, TX), followed by labeling with either Cy3 (pooled control RNA) or Cy5 (either tumor or TAHN pool) fluorescent cyanine dyes. Labeling was achieved by synthesizing the cDNAs in the presence of amino allyl dUTP (Sigma-Aldrich, St. Louis, MO) followed by chemically coupling of either Cy3 or Cy5 monofunctional dye (Amersham-Pharmacia Biotech, Arlington Heights, IL) to the cDNA. This process avoids biased incorporation of the dyes during reverse transcription.

Glass-slide-spotted-expression microarrays of the Qiagen Human Genome Oligo Set Version 3.0 (Qiagen) were used for this investigation. The arrays contained 37,123

transcripts, including 24,650 known genes, the rest being expressed sequence tags (ESTs) and controls. The design of these arrays is based on the Ensembl Human 13.31 Database (http://www.ensembl.org/) and on the Human Genome Sequencing Project. Equal parts of Cy3 and Cy5 labeled cDNAs were then combined and competitively hybridized to the microarray slides using the GeneTAC Genomic Solutions machine and protocol (Genomic Solutions Inc, Ann Arbor, MI). Following hybridization and washing, the slides were scanned at 532nm and 635nm using the Axon 4000A scanner (Axon Instruments, Union City, CA), and the signal data was processed using Axon GenePix Pro 5 software (Axon Instruments). Fluorescence intensities of the Cy3 and Cy5 dyes were determined for each oligonucleotide spot, followed by visual inspection prior to importing into Acuity 3.0 (Molecular Devices, Sunnyvale, CA). This program was utilized to normalize the data and allow for comparison between the replicates using standard quality calls (background removal, linear regression ratio >0.6, signal to noise ratio >3.0). Only data passing these quality filters were utilized in the present analysis. Sample groups, i.e. tumor and TAHN pools, were run in triplicate hybridizations.

Quantitative (real time) reverse transcriptase PCR. Quantitative Real Time PCR (qRT-PCR) was used to verify the results of the microarray expression analyses. Samples from both the MA and the independent VA sets were individually analyzed in quadruplicate for each selected gene/primer set. Approximately 1 μg of RNA from the samples was converted to cDNA using the Retroscript™ RT Kit (Ambion) according to the manufacturer's protocol using random decamers. The cDNAs were subsequently diluted 1:5 for use in the PCR reactions.

Genes included in mRNA expression evaluation included early growth response protein 1 (EGR-1), tristetraprolin (TTP), testican, fatty acid synthase (FAS), tissue inhibitor of metalloproteinase 2 (TIMP2), and superoxide dismutase 2 (SOD2). mRNA levels were quantitated using the Sybr Green real-time PCR assay kit (Applied Biosystems, Foster City, CA) in a 25uL reaction, using 0.5uL of the diluted cDNA. Primers were used at a final concentration of 400 uM for both the forward or reverse in each reaction with the exception of EGR-1, for which the forward primer was used at a final concentration of 1 μmol, the reverse at a final concentration of 1.5 μmol in the PCR reaction. The primers' sequences are listed in Table 9. PCR reactions were carried out under the following cycling parameters: 95˚C for 10 minutes followed by 40 cycles of 95˚C for 15 seconds, and 60˚C for one minute using the Gene Amp® 7000 Sequence Detection System (Applied Biosystems). Baseline fluorescence was determined during cycles 6-15.

The levels of EGR-1, TIMP2, and SOD2 were determined using the ΔΔCt method, where the threshold of detection of the genes of interest were compared to a house keeping gene, either the TATA binding protein (TBP) (for EGR-1), or glyceraldehyde 3-phosphate dehydrogenase (GAPDH) (for TIMP2 and SOD2). This method was chosen because the amplification efficiencies of their primers were determined to be similar to the ones of the control transcripts. The remaining genes, i.e. FAS, TTP, and testican, were evaluated using quantitation compared to serial dilutions of plasmids carrying cDNAs for these transcripts. Expression level calculations were controlled by the PCR efficiency corrected comparative quantitation method. Plasmids containing FAS, TTP, testican, and TBP PCR fragments were constructed using the

pGem T-Easy vector (Promega Corporation, Madison, WI), and the PCR product

incorporation was verified by sequencing. The data was reported as relative expression of

genes of interest in tumor and TAHN RNA compared to expression levels in the pooled

control prostate RNA.

Statistics. qRT-PCR results obtained from the microarray and validation sets

were analyzed using JMP IN version 3.2.1 from Statistical Analysis Software (SAS;

Cary, NC). Differences in the means between tumor or TAHN and cancer-free samples

were analyzed using unpaired two sample *t*-test; differences between matched tumor and

TAHN samples were analyzed using paired two sample *t*-test; differences with $p < 0.05$

were considered statistically significant.

Results:

Microarray expression analysis. We report RNA expression levels as ratios of

Cy3/Cy5 signals for individual transcripts, where the Cy3 and Cy5 fluorescent cyanine

dyes were used to label cDNA from experimental (tumor or TAHN) and pooled cancer-

free control tissues, respectively. While a ratio of 1.0 would thus indicate no change in

expression compared to cancer-free controls, there is the possibility of dye bias due to

differential incorporation of Cy3 and Cy5 during cDNA synthesis, or due to differential

hybridization of Cy3- and Cy5-labeled cDNAs to target probes. To estimate the extent of

potential dye bias, we labeled paired aliquots of control cDNA from cancer-free prostatic

Table 6. Primers used for qRT-PCR validation of microarray experiments.

Gene	Forward Primer (5'-3')	Reverse Primer (5'-3')	Product (basepairs)
Gene of Interest			
EGR-1	GAGCAGCCCTACGAGCAC	AGCGGCCAGTATAGGTGATG	130
FAS	AGAACTTGCAGGAGTTCTGGGACA	TCCGAAGAAGGAGGCATCAAACCT	149
Testican	TGGAACCGCTTTCGAGACGATGAT	CACACACTTTGTGAGGGCTGCATT	124
TTP	GTTACACCATGGATCTGACTGCCA	AGTCCCTCCATGGTCGGATGG	86
TIMP2	TGCAATGCAGATGTAGTGATCAGG GC	GGGTTGCCATAAATGTCGTTTCCAG	80
SOD2	AGCATGTTGAGCCGGGCAGTGT	TGCTTCTGCCTGGAGCCCAGATAC	74
Loading Control			
TBP	CACGAACCACGGCACTGATT	TTTTCTTGCTGCCAGTCTGGAC	112
GAPDH	ACCACAGTCCATGCCATCAC	TCCACCACCCTGTTGCTGTA	70

tissues with Cy3 and Cy5, combined equal amounts of the preparations, and hybridized them to a microarray set. Fluorescence analysis revealed a mean Cy3/Cy5 ratio of 1.27 ± 0.35 standard deviation (SD), a median ratio of 1.22, and a coefficient of variation of 27.3% for all transcripts (Table 10). In contrast, the means $\pm$ SD and coefficients of variation determined for the TAHN and tumor experimental sets were 1.58 ± 0.61 and 38.6%, and 1.63 ± 0.75 and 46.1%, respectively. Statistical analysis for the distribution of values for all detected transcripts revealed significant differences ($p<0.05$) for the tumor and TAHN microarray data from the Cy3/Cy5 dye bias test (Table 7). While this result indicated a minimal dye bias for Cy3 fluorescent cyanine cDNA incorporation and/or target hybridization, we considered all transcripts in the experimental sets with an expression ratio of <1.27 as equally or under-expressed compared to normal cancer-free prostatic tissues in order to avoid false positive assignment of over-expressed genes. Consideration of the Cy3/Cy5 dye bias is important because we focused our analyses of the microarray expression experiments on over-expressed transcripts, since over-expression of a protein marker in TAHN tissues would be amenable to positive identification and could thus be used in diagnostic tests.

In the microarrays, 3769 transcripts were mutually expressed in both tumor and TAHN tissues, 1810 of which were expressed above the Cy3/Cy5 dye bias of 1.27. We plotted the expression levels for these mutually expressed transcripts and analyzed their correlation between tumor and TAHN tissues (graphically shown Figure 11). Logisticregression analysis indicated a correlation coefficient R^2 of only 0.09, indicating overall poor concordance of the expression levels between tumor and TAHN tissues. The majority of these transcripts, i.e. 94% were expressed at <2.0xSD of the mean expression

Table 7. Dye bias control. Cy3/Cy5 fluorescent dye bias control microarray hybridization compared to experimental set using tumor and matched tumor adjacent histologically normal (TAHN) tissues.

	TAHN	**Tumor**	**Cy3/Cy5 Dye Bias Test**
Mean[1] ± SD	1.58 ± 0.61	1.63 ± 0.75	1.27 ± 0.35
Median	1.49	1.51	1.22
Coefficient of Variation (%)[2]	38.6*	46.1*	27.3

[1] Mean ± standard deviation (SD) for all transcripts detected.

[2] * denotes significant difference ($p < 0.05$) from Cy3/Cy5 dye bias test.

(see Table 10) of all transcripts expressed in tumor and TAHN tissues (i.e. <3.13 and
<2.80, respectively), as shown in quadrant I of Figure 11.
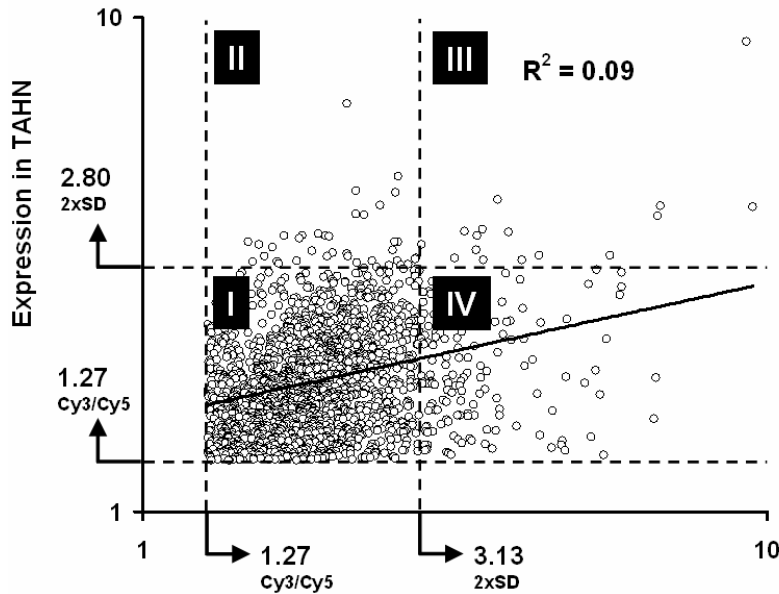
Figure 11. Analysis of microarray expression. Scatter plot of 1810 transcripts (open
circles) mutually expressed at >1.27 compared to cancer-free prostatic samples in tumor
and TAHN tissues as analyzed by microarray analysis (unknown transcripts included).
Expression in tumor and TAHN tissues is shown on the log-scaled x-axis and y-axis,
respectively. The Cy3/Cy5 dye bias and the 2xSD thresholds (as defined in Table 3) are
indicated by arrows and dotted lines. The solid line shows the best fit by logistic
regression analysis accompanied by correlation coefficient R^2. Quadrant I: Transcripts
expressed at <2.0xSD of the mean expression (see Table 3) of all transcripts expressed in
tumor and TAHN tissues (i.e. <3.13 and <2.80, respectively); quadrant II: Transcripts
expressed at >2.0xSD of the mean expression in TAHN and at >1.27 in tumor tissues;
quadrant III: Transcripts expressed at >2.0xSD of the mean expression in both TAHN
and tumor tissues; quadrant IV: Transcripts expressed at >2.0xSD of the mean expression
in tumor and at >1.27 in TAHN tissues.

We used over-expression in the tumor tissues as a guide for the selection and further analysis of transcripts in the TAHN tissues. Accordingly, we identified the transcripts that were over-expressed in the tumor tissues at >2.0xSD of the mean, i.e. all transcripts with a ratio >3.13. Omitting expressed sequence tags (ESTs) and unknown open reading frames (ORFs), this identified 120 known transcripts over-expressed in tumor tissues. Of these, 97 transcripts were also expressed in the TAHN tissues, 70 of which were also expressed at >1.27, i.e. above the Cy3/Cy5 dye bias threshold (quadrants III + IV, Figure 11). Eighty-three transcripts were over-expressed in the TAHN tissues at >2.0xSD of the mean, i.e. all transcripts with a ratio >2.80 (quadrants II + III, Figure 10). Due to space limits, we show the top 40 unique transcripts mutually over-expressed in tumor and TAHN tissues resulting from these analyses in Table 8. The number of mutually expressed and known transcripts at >2.0xSD for both tumor and TAHN tissues was 10 (quadrants III, Figure 10).

qRT-PCR validation of microarrays. As shown in Figure 8, microarray analysis indicated extensive heterogeneity of expression between tumor and TAHN tissues for the majority of transcripts. However, our microarray expression results represent mean values generated using pooled RNA populations. Therefore, it was important to estimate the extent of heterogeneity in individual samples. For this, we used qRT-PCR to test and validate the findings of the microarray expression analysis on selected transcripts in RNA samples of tumor and TAHN tissues compared to normal cancer-free prostate tissues. To better characterize the extent and heterogeneity of prostatic field cancerization in individual samples, we deliberately chose transcripts from above, below and at the

2.0xSD threshold of the mean in TAHN transcripts (i.e. ~2.8-fold over-expressed

compared to cancer-free tissues, as defined in Table 7). Early growth response protein 1

(EGR-1) represents the transcript most over-expressed (8.92-fold) in TAHN tissues and

has been previously implicated in prostate tumorigenesis (82-89). Its expression in tumor

tissue was 9.27-fold (Table 8). Testican, also known as SPOCK-1, was over-expressed at

4.29-fold and 1.73-fold in tumor and TAHN tissues, respectively. Testican has recently

been shown to be expressed in prostatic tissues (90). Fatty acid synthase (FAS) represents

an expected change in tumorigenesis of the prostate (91, 92) and was over-expressed at

5.31-fold and 1.93-fold in tumor and TAHN tissues, respectively. In contrast,

tristetraprolin (TTP) has not been previously reported to be associated with prostate

tumorigenesis and may thus represent a novel finding. It was expressed at 5.81-fold and

2.75-fold in tumor and TAHN prostatic tissues, respectively (Table 8). For control

purposes, we also included two transcripts that were equally or under-expressed in either

tumor or TAHN tissues, i.e. tissue inhibitor of metalloproteinase 2 (TIMP2) and

superoxide dismutase 2 (SOD2), expressed at 0.46-fold and 1.06-fold, and at 1.04-fold

and 0.42-fold in tumor and TAHN tissues, respectively. qRT-PCR validation was first

performed on the six individual RNA samples pooled and used in the microarray

expression analysis, the microarray (MA) set (Figure 12). In this analysis, the expression

levels were compared to 6 normal cancer-free prostate control samples. Although

variation was observed, mean expression of FAS, TTP, EGR-1 and testican in TAHN

tissues was significantly different from normal controls ($p < 0.05$; p range = 0.01-0.03).

Similarly, mean expression for these transcripts in tumor tissues was significantly

different from normal controls ($p < 0.05$; p range = <0.01-0.03). In contrast, and as

Table 8. Top 40 microarray transcripts. Top 40 transcripts mutually over-expressed in tumor and corresponding matched tumor adjacent histologically normal (TAHN) tissues compared to normal cancer-free prostatic tissue. [1] Gene identification number, Ensembl Human 13.31 Database (http://www.ensembl.org). [2] Cy3/Cy5 ratios of tumor or TAHN (Cy3) compared to cancer-free normal (Cy5) tissues. [3] The 4 transcripts evaluated by qRT-PCR (Figure 3) are in bold. [4] The shaded area represents transcripts above the 2xSD of the mean in TAHN tissues.

Gene ID[1]	Gene Description	TAHN[2]	Tumor[2]
H200019156	**Early growth response protein 1 (EGR-1)[3]**	**8.92[4]**	**9.27**
H200003548	Proto-oncogene protein c-Fos	4.13[4]	9.50
H200009720	Growth/differentiation factor 15 (GDF-15), macrophage inhibitory cytokine-1 (MIC1)	3.96[4]	6.68
H300013105	ETS-domain protein ELK-4	3.70[4]	3.28
H200005926	Metallothionein-IE (MT-1E)	3.68[4]	3.86
H300013389	Copine IV	3.62[4]	3.43
H300011237	Ergic-53-like protein precursor	3.37[4]	3.43
H300020290	Molecule possessing ankyrin repeats induced by lipopolysaccharide	3.09[4]	5.33
H300017466	Early response protein NAK1, TR3 orphan receptor	2.94[4]	4.03
H200000319	Aminopeptidase N	2.85[4]	5.85
H200019945	**Tristetraprolin (TTP)[3]**	**2.75[4]**	**5.81**
H300015296	Casein kinase I (CK1)	2.66	3.77
H200000676	Transcription factor Jun-D	2.64	3.45
H200006111	BTG2 protein	2.60	3.40
H200012441	Glandular kallikrein 1 precursor	2.58	4.06
H200020421	Paired immunoglobulin-like receptor beta	2.54	3.36
H300005679	Calreticulin precursor (CRP55), calregulin	2.45	4.79
H300014629	Tumor protein D52	2.43	3.88
H300022633	Similar to postmeiotic segregation increased 2-like 5	2.42	3.83
H300014182	Neprilysin	2.41	4.34
H300012307	Vascular endothelial growth factor A precursor (VEGF-A)	2.37	3.32
H300015765	Colorectal mutant cancer protein (MCC protein)	2.31	3.25
H300016106	Transcription factor EB	2.24	3.19
H300021922	Ubiquitin-protein ligase NEDD4-like	2.23	5.52
H300014306	HTPAP protein	2.23	4.08
H200014240	Poliovirus Receptor related protein (CD112 antigen)	2.10	3.71
H300004950	Claudin-4	1.97	4.09
H300017343	**Fatty acid synthase (FAS)[3]**	**1.93**	**5.31**
H200017342	Prostein protein	1.92	3.56
H300005700	Keratin, cytokeratin 8 (CK 8)	1.90	3.31
H300012280	Prostate specific antigen (PSA) precursor, kallikrein 3	1.89	3.15
H200003843	Diamine acetyltransferase	1.87	6.63
H300016780	Dolichyl-diphosphooligosaccharide-protein glycosyltransferas, 63 KD subunit	1.86	3.27
H200006197	NDRG1 protein	1.86	3.48
H300016292	Ubiquitin-conjugating enzyme E2-like	1.83	3.24
H200013682	X box binding protein-1 (XBP-1)	1.82	5.12
H300014868	KIAA0220-like protein (similar to nuclear pore complex interacting protein)	1.77	3.54
H300004833	**Testican (SPOCK-1)**	**1.73**	**4.29**
H200019551	Sialidase 1 precursor	1.72	5.40

expected, mean expression of the control transcripts TIMP2 and SOD2, which were equally or under-expressed in either tumor or TAHN tissues in the microarray experiments, was similar in TAHN and tumor tissues, as well as in normal controls ($p > 0.05$; p range = 0.27-0.70). Although not necessarily expected due to a higher degree of heterogeneity in cancerous tissues, expression of all of these transcripts was similar in TAHN and tumor tissues ($p > 0.05$; p range = 0.07-0.59), with the exception of FAS ($p = 0.02$). Thus, the results obtained with six individual RNA samples analyzed by qRT-PCR confirm the conclusions drawn from the analysis of pooled RNA by microarray expression analysis.

To corroborate these findings from the MA set, we also individually analyzed RNA from six independent tumors and patient matched TAHN tissues, the validation (VA) set. As in the MA set, mean expression of FAS, TTP, EGR-1 and testican in TAHN tissues was significantly different from normal controls ($p < 0.05$; p range = <0.01-0.03), demonstrating a consistent gene expression signature in TAHN tissues. In the VA set, mean expression of these transcripts in tumor tissues showed extensive variation when compared to normal controls, with EGR-1 and TTP showing significant and near significant differential expression ($p < 0.01$ and $p = 0.06$, respectively), and FAS and testican showing similar expression ($p = 0.10$ and $p = 0.27$, respectively). As expected, the control transcripts TIMP2 and SOD2 showed similar expression in TAHN and tumor tissues, and in normal controls ($p > 0.05$; p range = 0.28-1.00). Collectively, the qRT-PCR data (Figure 12) was in excellent agreement with the data from the microarrays, thereby indicating the occurrence of field cancerization for the selected transcripts in TAHN when compared to tumor and cancer-free tissues.

A FAS

B TTP

C EGR-1

D Testican

48
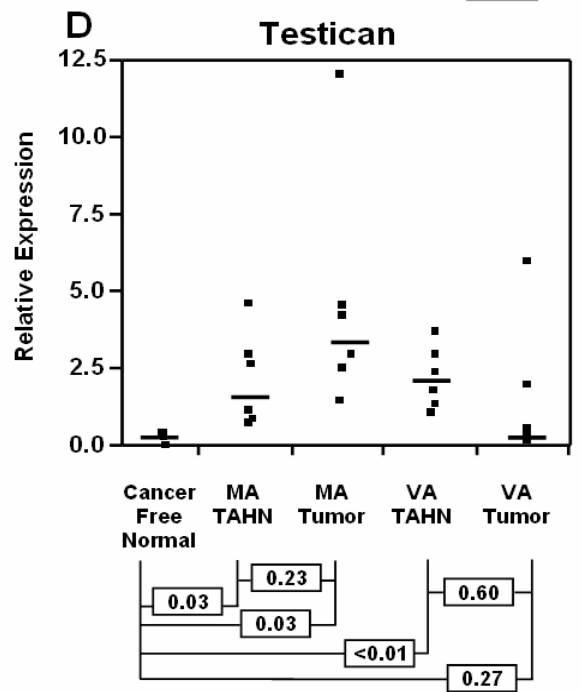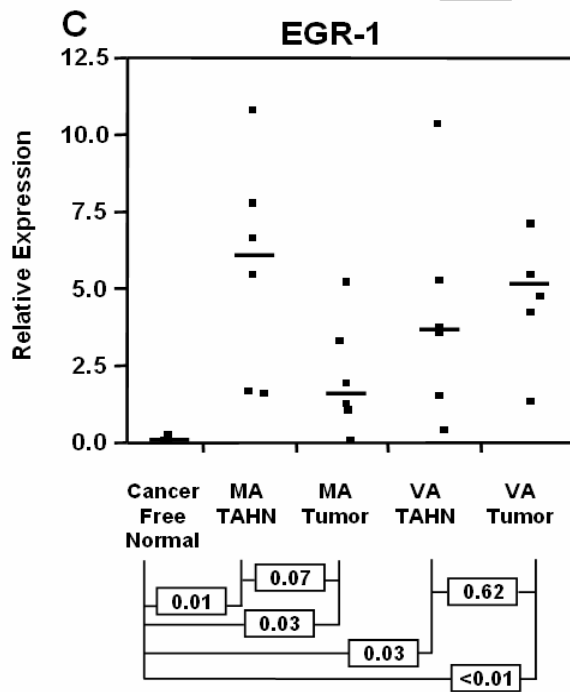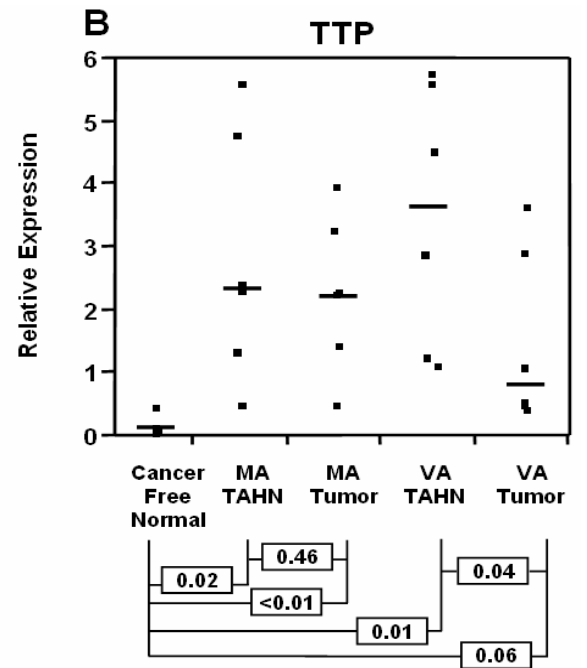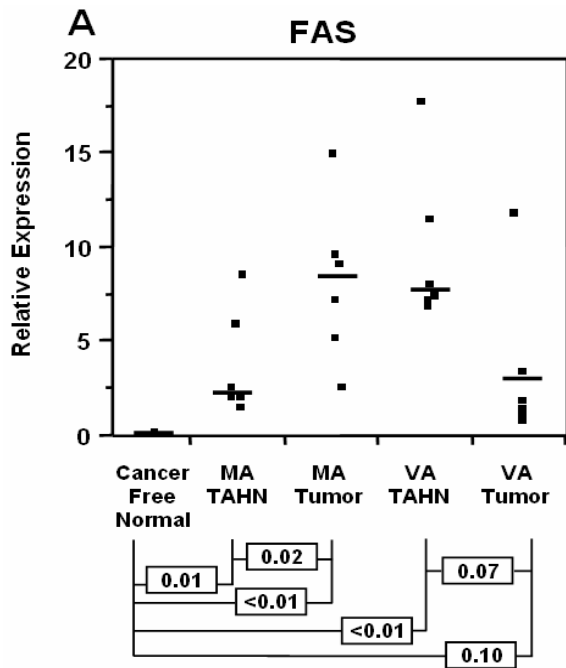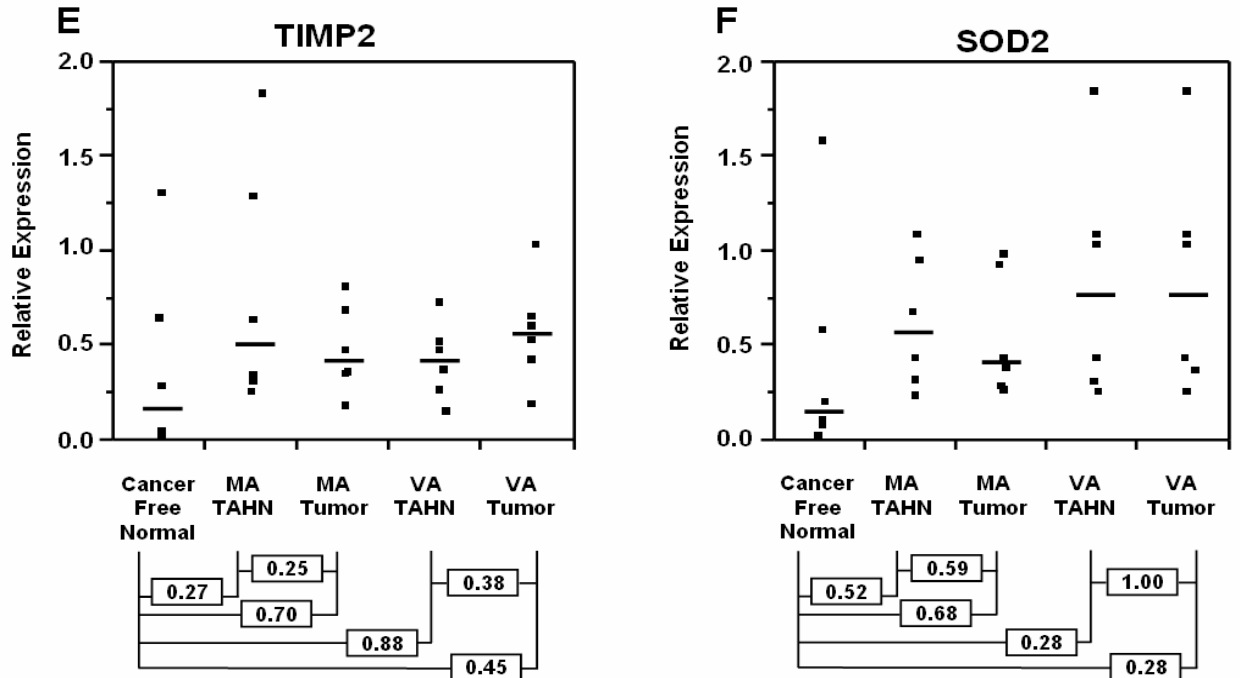
Figure 12. qRT-PCR validation of genes. RNA expression levels by qRT-PCR of FAS (A), TTP (B), EGR-1 (C), testican (D), and the control transcripts TIMP2 (E), and SOD2 (F) normalized to either GAPDH or TBP. The tissue groups are indicated on the y-axis (MA, microarray set; VA, validation set; TAHN, tumor adjacent histologically normal). Expression is shown on the y-axis relative to cancer-free normal prostatic tissues, dots represent the distribution, and the horizontal line indicates the median. The numbers represent the p-values for differences between indicated groups as determined by the unpaired (compared to cancer-free tissues) and paired (compared to matched tissues) t-test.

Discussion:

The major finding of this study is the occurrence of field cancerization in tumor adjacent histologically normal (TAHN) human prostatic tissues, as shown by microarray and qRT-PCR expression analysis of 12 mostly early stage (T2-T3) and low grade (Gleason sum 6-7) prostate tumors. In this study, we focused on the identification of transcripts that were

over-expressed in both tumor and TAHN prostatic tissues, as such transcripts encode proteins that define field cancerization. Proteins from field cancerized prostatic tissues may have important clinical applications, especially for the alternative or adjunct diagnosis of prostatic malignancy after inconclusive or false negative biopsy assessment. Dhir and colleagues have reported on the identification of early prostate cancer antigen (EPCA), a biomarker that is expressed throughout the prostate of individuals with prostate cancer but not in those without the disease, also indicating field cancerization (*21*). The authors of that study showed that EPCA staining by quantitative immunohistochemistry resulted in minimal overlap between samples from patients with prostate carcinoma and controls, and reported a sensitivity of 84% and a specificity of 85% in identifying individuals with prostate cancer >5 years earlier than currently used diagnostics.

Several expression studies have reported unique molecular signatures for prostate cancer by comparing cancerous to histologically cancer-free adjacent tissues and attempting to link the gene profiles to clinicopathological patient information such as stage and Gleason sum scoring (*93-100*). However, the use of matched tissues as appropriate controls has been questioned due to field cancerized cells harboring genetic and biochemical alterations (*101*). This is supported by our prior (*17, 38*) and present results. In contrast, few expression studies have reported molecular signatures and individual markers characteristic of prostatic TAHN tissues. Field cancerization is however evident at the genetic as well as the epigenetic level, as we have shown by altered telomeres in whole tissue TAHN extracts (*38*) and as shown by others by gene promoter methylation of APC, RARβ2, and RASSF1A (*20*). Field cancerization in

prostatic tissues is also evidenced by RNA/protein expression analysis (*40, 102*). In a similar study with a focus on signatures rather than single transcripts and without validation by qRT-PCR, Chandran and colleagues reported on up to 254 differentially expressed transcripts when comparing tumor associated matched tissues to cancer-free controls utilizing an Affymetrix platform of ~63,000 probes (*40*). Of note, the authors claim that the majority of these transcripts would not be identified as differentially expressed when compared to tumors. Due to different platforms, patient populations, and sample preparations, it is difficult to compare findings between studies. For example, while the exact distance of TAHN tissue from the tumor is not known in most published studies, we have carefully chosen a defined distance of 1cm. Despite differences, similarities reported by different groups corroborate the occurrence of field cancerization. Accordingly, Yu and colleagues have recently shown field cancerization in prostatic tissues at the expression level using gene chip technology on a set of 152 samples (*102*). Although these authors were mainly concerned with the comparison between tumor and matched tissues, they also reported expressional differences between prostatic TAHN and tissues from cancer-free control donors. Of interest in their study, the transcription factor c-Fos was over-expressed 2.55-6.80 and 4.67-6.67 in TAHN and tumor tissues, respectively. This is similar to our own findings of 4.13-fold and 9.50-fold over-expression in TAHN and tumor tissues, respectively (Table 12).

In the present study, we chose to use bulk tissue that was not microdissected in order to include both glandular (epithelial) as well as stromal (fibroblastic) compartments. While prostate adenocarcinoma is ultimately an epithelial disease, it is widely accepted that the stroma is involved in initiating, maintaining, and promoting a

malignant phenotype through inter-cell signaling (*103, 104*). These processes may also occur in TAHN tissues, as shown by Hanson and colleagues, who have reported promoter methylation for GSTP1, RARβ2, and CD44 in stromal cells associated with tumors (*104*). Additionally, this approach also demonstrates that the identified gene expression changes could potentially be identified in biopsy samples. In the present study, we pooled samples for the microarray analysis in order to minimize effects of sample heterogeneity. The authenticity of our findings, however, was confirmed by qRT-PCR using RNA from individual samples. Although heterogeneity from patient to patient was observed, data validity was corroborated in an additional independent set of patient samples.

Although not comprehensive, Table 8 indicates part of a signature that may be characteristic of prostatic field cancerized tissues. It is conceivable that many of the listed transcripts could have an important role in prostatic TAHN tissues, either a causative one as drivers of pre-malignancy or as a reaction to the presence of the tumor, or both. Among the highest over-expressed transcripts in TAHN tissues were EGR-1, c-Fos, and the growth/differentiation factor 15 (GDF-15), also called macrophage inhibitory cytokine-1 (MIC1). EGR-1 has been strongly implicated in prostate cancer (*82-89*) and regulates multiple target genes that in turn have a potential role in prostatic carcinogenesis and progression, such as epidermal growth factor receptor (EGFR), platelet derived growth factor (PDGF), and human telomerase reverse transcriptase (hTERT), thereby regulating a spectrum of cellular responses, including growth and growth arrest, survival and apoptosis, and differentiation and transformation (*105, 106*). The involvement of c-Fos as part of the transcription factor activator protein 1 (AP-1) that is activated downstream of many growth factors is supported by a large body of

literature on oncogenesis and metastasis (*107, 108*). GDF-15 (MIC1) is a member of the

transforming growth factor β (TGFβ) family and is known to be up-regulated in prostate

cancer (*109, 110*). In addition, increased levels of GDF-15 have also been correlated with

metastasis and the development of sclerotic bone lesions, which are typical for prostate

cancer (*110*). It has also been shown to contribute to chemotherapeutic drug resistance

(*111*).

However, to fully characterize the extent and heterogeneity of prostatic field

cancerization, in this study we also chose transcripts that were not the highest over-

expressed in TAHN tissues, such as TTP, FAS, and testican. TTP expression is not

specific to prostatic tissues. However, it is a ubiquitously expressed AU-rich element

(ARE) binding protein and a regulator of mRNA stability, including of pro-inflammatory

proteins, such as tumor necrosis alpha (TNFα) (*112*), which plays an important role in

prostate adenocarcinoma (*113*). It is possible that TNFα is produced by inflammatory

cells in TAHN tissues in agreement with the prominent role of inflammation as proposed

by De Marzo and colleagues (*114*). TNFα is a classical activator of the nuclear factor

kappa B (NFκB) pathway which is constitutively activated in prostate cancer with

prominent downstream targets that support an activated cellular state, including EGR-1

(*105, 115*). FAS has been termed a "metabolic oncogene" and may reflect a prostate

cell's energetic switch to a more anaerobic yet more reductive physiologic state, which is

a hallmark of prostate cancer progression (*91, 92*). In addition, FAS has been shown to

positively affect NFκB nuclear translocation in cancer cells leading to an anti-apoptotic

effect (*116*). Finally, testican (SPOCK-1) belongs to the fibulin protein family of

extracellular matrix proteins which influence cell adhesion and migration, and have thus

been associated with progression of several cancer types (*117*), including prostate cancer, in which it has recently been shown to be up-regulated (*90*).

Collectively, our data supports the occurrence of field cancerization in prostatic tissues and warrants further investigations into its underlying mechanisms and potential clinical use of representative transcripts towards an improved prostate cancer detection and patient outcome.

Chapter 5

TC in matched biopsy and prostatectomy tissues

Specific Aim: Evaluate and compare the relationship between disease progression and telomere content (TC) in cancerous and histologically normal prostate tissues obtained from biopsy and prostatectomy.

Introduction: Telomeres are the protein-nucleic acid structures that stabilize and protect the ends of the chromosomes. Normally 1-2,000 repeats of the hexanucleotide sequence TTAGGG are found capping the DNA strands. Telomeres are shortened by 40-50 nucleotides per round of replication due to steric inhibition by the DNA polymerase binding to the leading strand during replication. When telomeres reach a critical length senescence or apoptosis results in order to protect the integrity of the DNA of that cell. However, multiple mechanisms in the cancerous cell, for example p53 and Rb mutations, can bypass these checkpoints allowing further cell division. If neither senescence nor apoptosis occurs and the telomeres continue to shorten, chromosome fusion, breakage, and recombination ensues. Unchecked, these events lead to cell death, but in cancer cells, telomeres are stabilized by the activation of telomerase, the enzyme that lengthens telomeres.

Because telomerase is frequently activated in cancer cells, it follows that telomere length of these cells will be different from normal, healthy cells, and this has indeed been observed to be the case. Our laboratory has developed an assay to measure telomere content (TC), a surrogate for telomere length, to evaluate telomeres of cancer and normal

cells (*39, 47*). Additionally, our laboratory has used the TC assay to investigate field effect in the tumor adjacent histologically normal tissues of breast and prostate cancer. These studies have established that the telomeres of tumor cells are abnormal compared to disease-free cells, that shorter telomeres are associated with a poorer outcome, and that a field of genetically altered cells surrounds a tumor (*17, 34, 37-39*).

Based on our preliminary studies, we have proposed that TC predicts disease-free survival in men with prostate cancer (Figure 4). To confirm and refine this finding, we conducted a retrospective study comparing TC in cancerous and histologically normal tissues from patient matched biopsy and prostatectomy specimens in which the patients differ in recurrence outcome. The objective of this study was to determine whether TC measured in tissue obtained by biopsy has diagnostic or prognostic value. Additionally, this study investigated the relationship between TC in patient tissues obtained at biopsy and subsequent prostatectomy.

Materials and Methods

Study cohort: The cases for this study were provided by Cooperative Prostate Cancer Tissue Resource (CPCTR) in Pittsburgh, Pennsylvania. Slides provided included a TAHN and tumor prostatectomy sample, and a cancerous tissue from biopsy; a portion of the cases also included a histologically normal biopsy. For the purpose of this study, sample sets were initially required to include all four tissue samples, although not all samples yielded usable DNA. A total of 56 cases were chosen for analysis, of which 8 were African American and 48 were Caucasian. Gleason sum scores ranged from 5 to 8,

with the majority being either Gleason Score 6 (22 cases) or 7 (30 cases). The median age at time of prostatectomy was 63.5 years, with a range 47 to 79 years (Table 9). Of the 56 cases, 25 cases had recurrence as defined by PSA recurrence, and 31 cases did not recur (Table 10).

Six prostate samples from cancer-free controls (sudden death cases) were obtained from the National Cancer Institute Cooperative Human Tissue Network (CHTN; Nashville, TN), stored at -70°C, and subjected to DNA extraction and histological review. The latter confirmed these samples to be free of both cancer and BPH. The median age of this set was 44.5 years, with a range of 26-79 years.

DNA Isolation: DNA was isolated from formalin fixed, paraffin embedded tissue mounted on glass slides. Sections were 10 μm thick, unstained, and were derived from either needle core biopsy or prostatectomy. If the specimen was from a biopsy, four slides were used, if the sample was from a prostatectomy, two slides were used. Slides were deparaffinized and rehydrated using xylene and decreasing concentrations of ethanol. The tissue was scraped off the slide for DNA isolation using a commercial isolation kit (Qiagen DNEasy Kit, Valencia, CA)

Quantification of DNA: DNA isolation was followed by quantitation with the fluorescent dye, PicoGreen (Quant-iT™ Picogreen ® dsDNA Kit, Molecular Probes, Eugene, OR) to determine the amount of double stranded DNA isolated according to the

Table 9. **Characteristics of the Telomere Content study cohort**.

Patient demographics (cases)	
Caucasian	48
African American	8
Age at Prostatectomy (years)	
Range	47-79
Median	63.5
Mean	62.9
Gleason Score	
5	2
6	22
7	30
8	2
Stage	
T2a/b	46
T3	10
% gland occupied	
<5%	21
5-25%	29
>25%	4

Table 10. Recurrence/follow up information of the Telomere Content study.

	Number of patients	Median (in months)	Mean	Min	Max
Recurrence	25	27	35.8	14	109
No Recurrence	31	62	58.8	17	134

manufacturer's protocol. Lambda phage DNA provided with the kit was used for the

control DNA to generate a standard curve. The control DNA standards and samples were

evaluated by excitation at 480nm and measuring the output at 520nm on a Luminescence

Spectrometer LS50 (Perkin Elmer, Boston, MA). Sample DNA concentrations were

calculated from the equation of the best-fit line generated from the standard control DNA.

Telomere Content assay: Our laboratory has previously developed an assay to

determine telomere content, an established surrogate for telomere length (*37, 39, 47*).

Patient samples were prepared at DNA concentrations ranging from 5-20 ng in TE buffer

in quadruplicate. A standard curve ranging from 0-40 ng was prepared using placental

DNA. Denaturing solution (0.05M NaOH, 1.5M NaCl) was added to the samples before

placing in a water bath at 56° C for 40 minutes. The samples were then removed from the

water bath and neutralizing solution (0.5M Tris, 1.5M NaCl) was added to the samples.

Samples were then loaded onto the prepared Tropilon-Plus Positively Charged Nylon

Membrane (Tropix, Bedford, MA) in the slot blot apparatus (Minifold® Slot-Blot

System, Schleicher & Schuell, Keene, NH). Membrane preparation included two washes

under vacuum with neutralizing solution. Following application of the samples under

vacuum, the blot was washed again with neutralizing solution and placed in 5X SSC for

10 minutes. The membrane was then air-dried and UV cross-linked with 1200 mJ (UVP,

Upland, CA). Next, the blot was wet with 0.25M sodium phosphate buffer, and then pre-

hybridized in a glass hybridization bottle (Bellco Glass, Vineland, NJ) in pre-

hybridization buffer (7% SDS, 0.25M sodium phosphate buffer, 0.001M EDTA, and 1X

Denhart's Solution) for 1 hour at 60° C. Following pre-hybridization, hybridization

buffer (7% SDS, 0.25M sodium phosphate buffer, and 0.001M EDTA) with 500 pmols of telomere probe was applied to the blot. The telomere probe is a telomere-specific FAM 3' end labeled probe: 5'-(TTAGGG)$_4$ -6-FAM-3' (IDT, Coralville, IA). The blot was incubated overnight at 60° C in this solution. Following hybridization, the blot was washed 2 times in 2X SSC/1% SDS for 5 minutes, 2 times in 1X SSC/1% SDS for 15 minutes, and 2 times in 1X SSC for 5 minutes, respectively. Washes were carried out at room temperature with the exception of the 1X SSC/1% SDS wash, which was done at 60° C. All washes were carried out in glass hybridization bottles.

In order to detect the fluorescein probe using the Southern Star™ chemiluminescent kit (Tropix, Bedford, MA), the blot was blocked (1X PBS, 2% I Block reagent (Tropix, Bedford, MA), and 0.1% Tween 20) for 40 minutes at room temperature. This was followed by incubation in fresh blocking buffer with 0.5 uL of anti-fluorescein-AP Fab fragments antibody (Roche Diagnostics Corporation, Indianapolis, IN) for 2 hours at room temperature. The blot was washed for 5 minutes at room temperature with fresh blocking buffer, then washed 3 times for 5 minutes with wash buffer (1X PBS and 0.1% Tween 20), also at room temperature. Next, the blot was incubated in 1X assay buffer (Tropix, Bedford, MA) 2 times for 2 minutes each at room temperature to optimize alkaline phosphatase activity. Finally, the blot was incubated with CDP-Star® chemiluminescent substrate (Tropix, Bedford, MA) for 5 minutes and was then blotted dry and sealed into plastic wrap for exposure to Hyperfilm ECL-Chemiluminescence film (Amersham Biosciences, Buckinghamshire, England).

Following exposure, films were developed (Konica Medical Film Processor-model QX-70) and scanned (Hewlett-Packard ScanJet ADF). The digitized images were

analyzed using Nucleotech Gel Expert Software 4.0 (Nucleotech, San Mateo, CA) in order to determine the intensity of telomere hybridization signal. The TC values obtained from each mass of the placental DNA standards were plotted and used to generate a linear line equation. Sample telomere content is expressed as the ratio of the actual TC measured for each sample mass to the TC predicted by the line equation, expressed as a percentage.

Statistical Design: All statistical analysis was carried out using JMP IN version 3.2.1 from Statistical Analysis Software (SAS; Cary, NC). Differences in the means between histologically normal tissue from biopsy, cancerous tissue from biopsy, TAHN, and Tumor to cancer-free samples were analyzed using Student's *t*-test; differences with $p < 0.05$ were considered statistically significant.

Results:

Telomere content in the six normal prostate tissues ranged from 94-121%. This agrees well with the previously reported range of 75-143%, that defines TC in 95% of 70 normal tissue samples from multiple organ sources (*17*).

Telomere content of the histologically normal tissue from biopsies (*n*=15) ranged from 25-217%, with a mean of 86% and median of 66%. Cancerous tissue from biopsy telomere content (*n*=40) ranged from 7-220%, with a mean of 74% and a median of 66%. The range for TAHN (*n*=33) was 17-355%, with a mean of 77% and a median of 58%. Finally, Tumor (*n*=39) ranged from 11-360% with a mean of 66% and a median of 59%

(Figure 13). The median of all sample groupings fell below the experimentally determined

normal telomere content range.
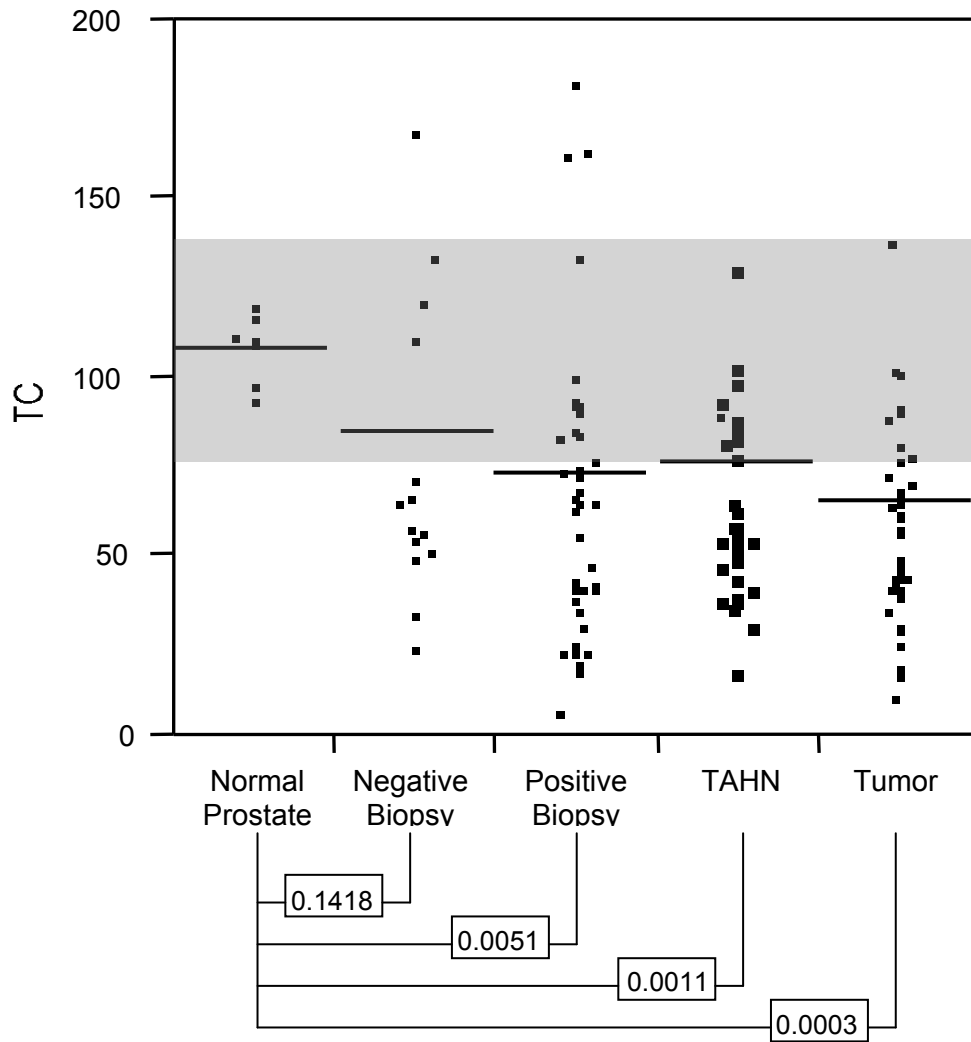
Figure 13. Telomere Content of samples by tissue source. The gray box indicates the
95% range of normal tissues as determined experimentally. Boxes contain the *p*-values
between the sample groups (Student's *t*-test).
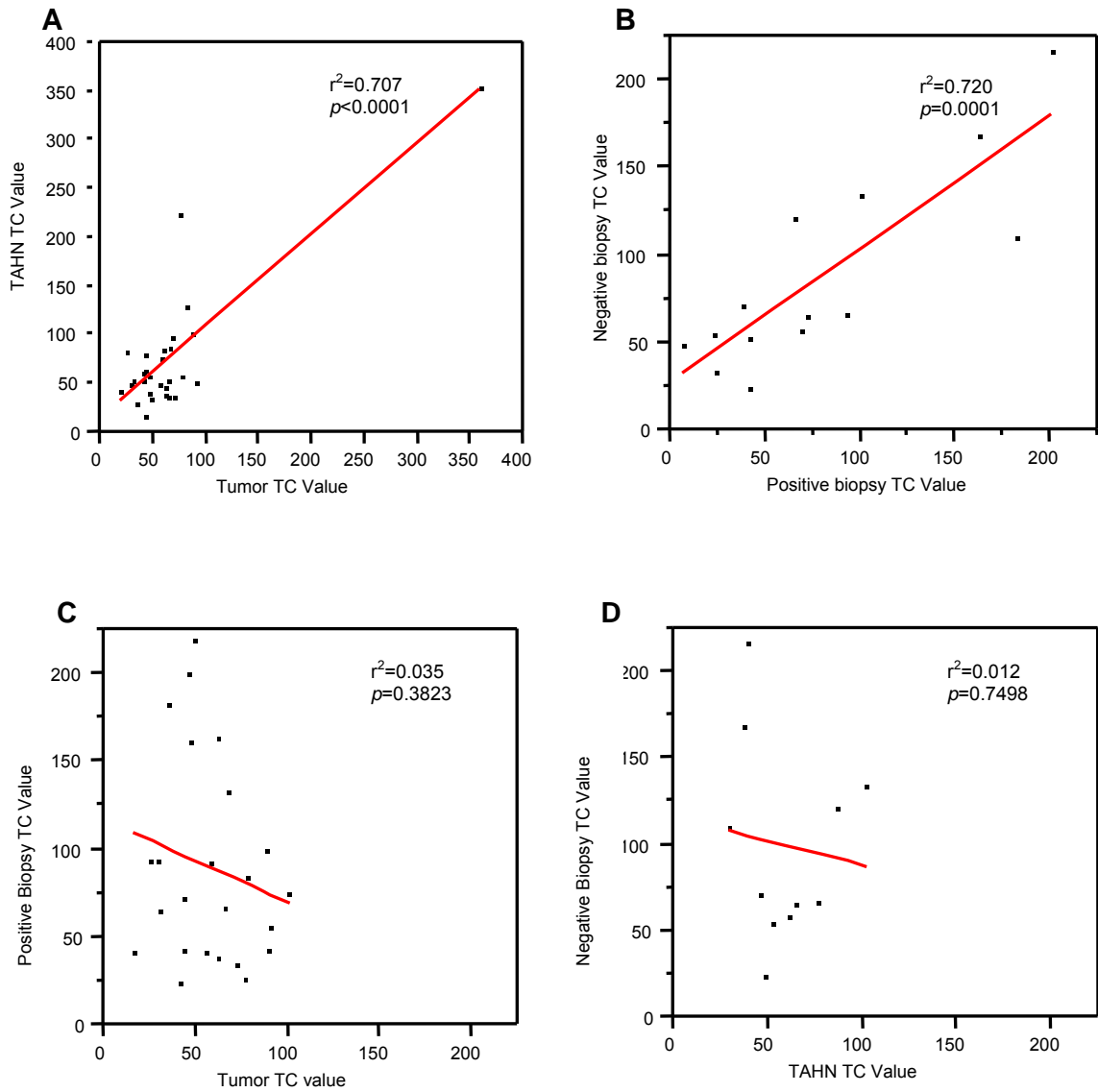
Figure 14. Correlation of samples by tissue source. Paired samples by prostatectomy or biopsy, and compared by relative tissue type. Panel A shows the TC relationship between TAHN and Tumor tissues. Panel shows the TC relationship between Negative and Positive Biopsy tissues. Panel C shows the lack of TC correlation between Positive Biopsy and Tumor tissues. Panel D shows the lack of TC correlation between Negative Biopsy and TAHN tissues.

TC in TAHN and Tumor tissues in patient matched samples was strongly correlated ($n=29$, $r^2=0.707$, $p=<0.0001$, Figure 13) as was TC in TAHN and cancerous tissues from patient matched biopsy specimens ($n=14$, $r^2=0.720$, $p=0.0001$). Surprisingly, TC was neither correlated in TAHN tissues from patient matched biopsy and prostatectomy ($n=11$, $r^2=0.012$, $p=0.7498$), nor cancerous tissues from patient matched biopsy and prostatectomy ($n=24$, $r^2=0.035$, $p=0.3823$) (Figure 14).

Discussion:

The results of these studies are similar to those reported previously for cancerous breast samples (*17, 34, 38*) and cancerous prostate tissues (*37, 38*). Our prior studies demonstrated that TC in tissues obtained from radical mastectomy and prostatectomy was significantly reduced compared to disease-free prostate and breast tissues. More importantly, these studies also found that the histologically normal tissue adjacent to the tumor had significantly reduced TC compared to disease-free tissues.

The current study confirmed those findings in prostatectomy tissue, and extended them to biopsy tissue. As expected, the findings were similar in the biopsy tissues to those in prostatectomy tissues. Specifically, cancerous tissue from biopsy TC was significantly reduced compared to disease-free tissue, and histologically normal tissue from biopsy tissue was also significantly reduced in matched patient samples. These findings indicate that TC in biopsy tissues may be informative of the presence of prostate cancer. These findings indicate that it may be possible to detect abnormalities in biopsy tissue indicative of cancer, potentially avoiding repeated biopsies and leading to earlier treatment in cases that would otherwise have been missed on the basis of histology.

The matched biopsy and prostatectomy samples used in this study enabled, for the first time, an evaluation of two separate time points in patient matched samples. The results demonstrate that TC in tissues from biopsy and prostatectomy specimens is informative, regardless of histology. However, TC was not correlated between paired histologically normal or cancerous biopsy and prostatectomy specimens. There are two possible explanations for this: a) Temporal alterations and/or b) spatial alterations. It is possible that telomere length is highly dynamic and constantly changing. The time between biopsy and prostatectomy was unknown for the samples in this study, so it is possible that the findings reflect ongoing changes in the abnormal cells. It is also possible that the differences are due to the physical location within the prostate of the sample collected. Biopsy samples are taken in a grid pattern and only sample a small portion of the prostate, however, the general sampling area changes very little from patient to patient. Tissues collected from prostatectomy specimens can come from any location within the prostate. Additionally, unpublished data from our laboratory has found a high level of heterogeneity within the prostate itself regarding TC. Based on that previous work revealing a range of TC variation throughout the cancerous prostate and the findings of TC correlation in prostatectomy specimens found by this study, it is more likely that the TC correlation observed is due to spatial variation. However, temporal effects cannot be ruled out, due to the lack of data regarding time between biopsy and prostatectomy. More research will be needed to further elucidate this point.

Chapter 6

Allelic Imbalance in matched biopsy and prostatectomy tissues

Specific Aim: Evaluate and compare the relationship between disease progression and allelic imbalance (AI) in cancerous and histologically normal prostate tissues obtained from biopsy and prostatectomy.

Introduction: Despite increased public awareness about prostate cancer and Prostate-Specific Antigen (PSA) testing, prostate cancer rates continue to increase. This is largely a direct result of increased detection. However, increased testing rates have also demonstrated that PSA testing is not as reliable as once thought. While the current limit to normal PSA levels is 4ng/mL, 20-30% of men with clinically confirmed prostate cancer have normal PSA levels (*4*). To compound the problem, benign processes, such as BPH and prostatitis, can elevate PSA levels, PSA does not differentiate between cancerous and benign processes, and some men normally produce more PSA (*4, 118*). Most frightening to cancer patients following treatment without prostatectomy, PSA levels may actually rise temporarily depending on the type of treatment, causing great distress (*7*). Yet, to date, no better biomarker has been found, either for detecting cancer or for its prognosis (*4*). Based on our preliminary studies, we propose that AI, like TC, predicts disease-free survival in men with prostate cancer. To confirm and refine this finding, we proposed first to conduct a case-controlled study in which the patients differ in disease stage at time of diagnosis and recurrence outcome. These experiments determined if AI predicts disease recurrence independent of stage at diagnosis. Based on

preliminary studies suggesting that AI can predicts disease-free survival in men with differing pathological grades, we also proposed to determine if AI is suitable for diagnosis and staging of prostate cancer, both in prostatectomy and, more importantly, biopsy tissues. While a highly specific panel of microsatellite markers could be developed, it is clear from our previous studies of breast and prostate tumors that genomic instability is widespread and nonspecific. Because of this, a nonspecific test, previously described (*17*), is being used.

Based on our preliminary studies, we proposed that AI, like TC, predicts disease-free survival in men with prostate cancer (Figure 4). To confirm and refine this finding, we conducted a retrospective study comparing AI sensitivity and specificity in both biopsy and prostatectomy tissues to patient outcome, in which the patients differed in disease stage at time of diagnosis and recurrence outcome. These experiments investigated whether AI could be used to predict disease recurrence independent of stage at diagnosis. Based on preliminary studies suggesting that AI can predict disease-free survival in men with differing pathological grades, we also proposed to determine if AI is more sensitive than PSA as a marker in prostate cancer diagnosis and staging.

Methods and Experimental Design

Specimen Acquisition: Slides were provided by the Cooperative Prostate Cancer Tissue Resource in Pittsburg, Pennsylvania. Tissues provided included a malignant prostatectomy sample, a benign prostatectomy sample, a cancerous biopsy sample and a histologically normal biopsy sample where available. For the purpose of this study,

sample sets were required to include all four tissue samples, although not all samples yielded usable DNA. The study was comprised of a total of 56 cases, of which 49 were Caucasian and 7 were African American. The range of ages at prostatectomy was 47-79 years, with a median of 63 years, a mean of 62 years. Gleason scores ranged from 5-8, however only 2 were Gleason score 5 or 8. Twenty-two cases were Gleason score 6, and the remaining 30 cases were Gleason score 7. Of the cases, 45 were staged T2a or b, and 11 were stage T3a or b (Table 11). Twenty-five cases recurred, with the median time to recurrence being 27 months, and 31 cases remained disease-free at a median time of 63 months (Table 12).

Nine prostate samples from cancer-free controls (sudden death cases) were obtained from the National Cancer Institute Cooperative Human Tissue Network (CHTN; Nashville, TN), stored at -70˚C, and subjected to DNA extraction and histological review. The latter confirmed these samples to be cancer-free and also free of BPH. The mean age of this set was 36.6 years, the median was 43 years of age, and the range was 0-79 years.

DNA isolation: DNA was isolated as described in Chapter 5.

Allelic Imbalance Determination in Prostate Tumors: Allelic imbalance will be evaluated using a PCR based assay similar to that described previously (*45, 46*), developed in our laboratory. The AmpFlSTR® kit (Applied Biosystems, Foster City, CA) contains reagents that amplify 16 different short tandem repeat (i.e. microsatellite) loci within a single multiplex reaction. These 16 loci are located randomly throughout the

Table 11. Patient cohort of the Allelic Imbalance study.

Patient demographics (cases)	
Caucasian	49
African American	7
Age at Prostatectomy (in years)	
Range	47-79
Median	63
Mean	62.68
Gleason Score	
5	2
6	22
7	30
8	2
Stage	
T2a/b	45
T3a/b	11

Table 12. Recurrence data among the Allelic Imbalance study cohort.

	Number of patients	Median time to outcome (months)	Mean (months)	Min (months)	Max (months)
Recurrence	25	27	35.85	14	109
No Recurrence	31	62	59.48	17	134

genome and include Amelogenin, CSF1PO, D2S1338, D3S1358, D5S818, D7S820, D8S1179, D13S317, D16S539, D18S51, D19S433, D21S11, FGA, TH01, TPOX, AND vWA. The amplicons from this reaction are separated by capillary electrophoresis and histograms of the fluorescently labeled products are generated. Approximately 1ng of DNA will be amplified in a standard 25 µl reaction mix according to the manufacturer's protocol. In each reaction there will be 10 µl of the reaction mix, 5 µl of the "Identifiler" Primer Set and 2.5 U of AmpliTaq Gold DNA polymerase (Applied Biosystems, FosterCity, CA). Cycling conditions include an initial denaturation at 95ºC for 11 min followed by 30 cycles of 1 min at 94ºC, 1 min at 59ºC, and 1 min at 72ºC, with a final extension of 60 min at 60ºC. PCR products will be resolved by capillary electrophoresis and detected using an ABI Prism 377 DNA Sequencer (Perkin Elmer, Foster City, CA).

Two possible outcomes exist for this assay. When a locus is homozygous, *i.e.* instances when a single peak is observed, a determination of loss of heterozigosity cannot be made as there is no "normal" comparison population. Alternatively, when a locus is heterozygous, *i.e.* the instances when two peaks are observed, the ratio of the peak heights is used to determine if a sample is heterozygous or if it is imbalanced. Based on our previously published studies, a site of allelic imbalance will be called when the ratio is greater than 1.60 (*17*).

Statistical Design: JMP IN version 3.2.1 from Statistical Analysis Software (SAS; Cary, NC) was used to analyze the study results. Differences in the means between Negative Biopsy, Positive Biopsy, TAHN, and Tumor tissues and cancer-free samples

were analyzed using the Student's *t*-test; differences with p<0.05 were considered statistically significant.

Results:

Allelic Imbalance was investigated in a total of 143 samples, 24 histologically normal biopsy samples, 41 cancerous biopsy samples, 31 TAHN samples, 38 Tumor samples, and 9 disease-free prostate samples. Seven of the normal samples had zero sites of AI, and 2 samples had 1 site of AI for an average of 0.22 sites of AI per sample. These results were consistent with our previous study of 118 normal tissues from various organs. This demonstrated that approximately 75% and 25% of normal tissues have no sites and one site of AI, respectively. Only one sample (0.8%) had 2 sites of AI. Overall, there was an average of 0.27 sites of AI per sample (*48*).

In contrast to the normal tissues, the histologically normal biopsy samples had an average of 1.92 sites of AI (*p*=0.0049), while the cancerous biopsy samples had an average of 1.61 sites of AI (*p*=0.0001). Among the prostatectomy samples, TAHN tissues had an average of 2.23 sites of AI (*p*=0.0006) and the Tumor tissues had 2.71 sites of AI (*p*=<0.0001) on average (Figure 14).

Figure 14. Allelic Imbalance. Allelic Imbalance of study cohort compared to normal prostate tissues. Boxes indicate significance as determined by the Student's *t*-test.

With multiple patient matched specimens, the opportunity arose to investigate clonality between the field and the tumor cells populations. Additionally, because the patient cases included both biopsy and prostatectomy specimens, clonality could also be looked at over time, *i.e.* between biopsy and prostatectomy. We hypothesized that if a

clonal relationship existed between the specimens, there would be matched sites of AI between them, *i.e.* the same locus would be imbalanced in both the TAHN and Tumor specimens. Analysis of the actual sites of AI was performed on three sub-populations: paired biopsy samples, paired prostatectomy samples, and matched samples with data for both biopsy and prostatectomy samples, resulting in groups of 4 pairs, 10 pairs, and 18 sets, respectively. Sites of AI in the patient matched cancerous biopsy specimens were compared to the histologically normal biopsy specimens and sites of AI found in patient matched tumor tissue were compared to TAHN (Table 14). While the four sets of matched histologically normal and cancerous biopsies did not contain and matched sites of AI, the 10 patient matched prostatectomy samples had 7 common sites of AI out of 17 possible instances (41.2%). In the 18 cases with all 4 tissues types providing data (Table 15), there were 12 instances of matched AI sites in the biopsy tissues out of 33 instances of AI in the Negative Biopsy samples (36.4%); 11 matched sites existed with 46 possible matches (23.9%) between tumor compared with TAHN. Nine sites of AI were found in 3 of the 4 tissue types (*i.e.* cancerous biopsy, TAHN, and tumor specimens), and 3 of these cases had 2 instances of the conserved sites. Most interesting was the finding of 2 cases with a conserved site of AI in all 4 samples.

Discussion:
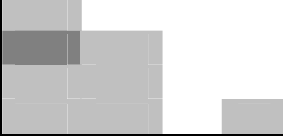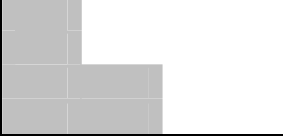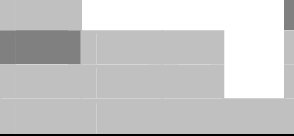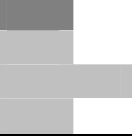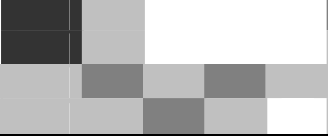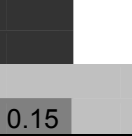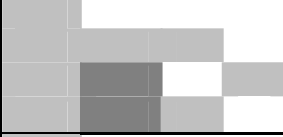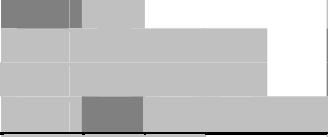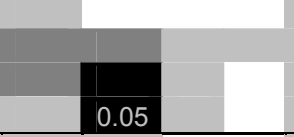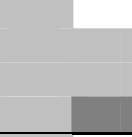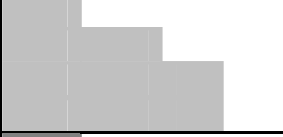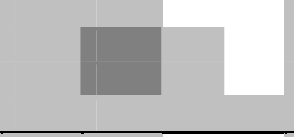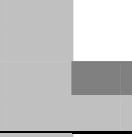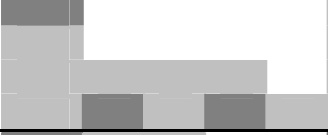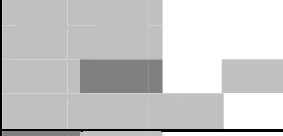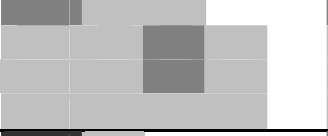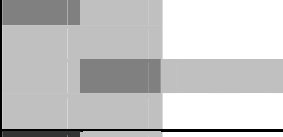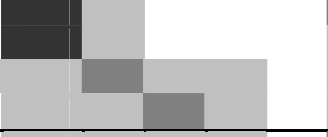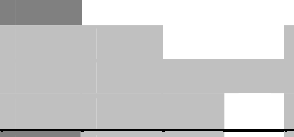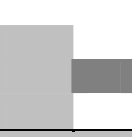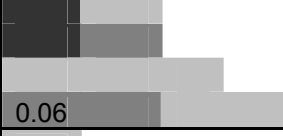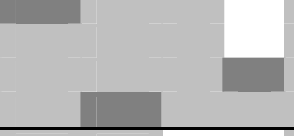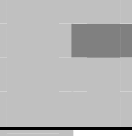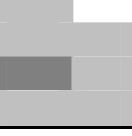
Genomic instability is a common occurrence in cancer (*13, 15, 119*). Instability can be reflected in loss of heterozigosity, and so other studies have endeavored to determine if loss of heterozigosity at specific loci can be used to detect prostate cancer (*120, 121*). However, this approach assumes that the genomic changes are

Table 14. Clonality of allelic imbalance in paired specimens. Matched samples, either Negative and Positive Biopsy or TAHN and Tumor. The lightest gray boxes indicate a heterozygous or non-informative allele, the darker gray boxes indicate a site of imbalance. The darkest boxes indicate a matched site of imbalance in the two tissue types. The numbers at the left of the table indicate the case number. The following column notates the sample type. The numbers across the top correlate to the allele tested. Amelogenin was not included in the table as the entire cohort is male. 1-D8S1179; 2-D21S11; 3-D7S820; 4-CSF1PO; 5-D3S1358; 6-THO1; 7-D13S317; 8-D16S539; 9-D2S1338; 10-D19S433; 11-vWA; 12-TPOX; 13-D18S51; 14-D5S818; 15-FGA.

		1	2	3	4	5	6	7	8	9	10	11	12	13	14	15
1	Neg Bx															
	Pos Bx															
2	Neg Bx															
	Pos Bx															
3	Neg Bx															
	Pos Bx															
4	Neg Bx															
	Pos Bx															
5	TAHN															
	Tumor															
6	TAHN															
	Tumor															
7	TAHN															
	Tumor															
8	TAHN															
	Tumor															
9	TAHN															
	Tumor															
10	TAHN															
	Tumor															
11	TAHN															
	Tumor															
12	TAHN															
	Tumor															
13	TAHN															
	Tumor															
14	TAHN															
	Tumor															

Table 15. Clonaity of allelic imbalance in matched biopsy and prostatectomy specimens. Cases including all four sample types: Negative Biopsy, Positive Biopsy, TAHN, and Tumor tissue. The lightest gray boxes indicate sites of heterozigosity or homozygous/non-informative alleles. Darker gray boxes indicate sites of allelic imbalance. The darkest boxes indicate paired sites of allelic imbalance between either Negative Biopsy and Positive Biopsy tissues or TAHN and Tumor tissues. In cases with three common sites of imbalance between the sample types, the number indicates the likelihood of imbalance between the three sample types. The numbers at the left of the table indicate the case number. The following column notates the sample type. The numbers across the top correlate to the allele tested. Amelogenin was not included in the table as the entire cohort is male. 1-D8S1179; 2-D21S11; 3-D7S820; 4-CSF1PO; 5-D3S1358; 6-THO1; 7-D13S317; 8-D16S539; 9-D2S1338; 10-D19S433; 11-vWA; 12-TPOX; 13-D18S51; 14-D5S818; 15-FGA.

		1	2	3	4	5	6	7	8	9	10	11	12	13	14	15
15	Neg Bx															
	Pos Bx															
	TAHN															
	Tumor															
16	Neg Bx															
	Pos Bx															
	TAHN										0.12					
	Tumor					0.08										
17	Neg Bx															
	Pos Bx															
	TAHN															
	Tumor															
18	Neg Bx															
	Pos Bx															
	TAHN															
	Tumor										0.01					
19	Neg Bx															
	Pos Bx															
	TAHN															
	Tumor											0.08			0.22	
20	Neg Bx															
	Pos Bx															
	TAHN															
	Tumor															
21	Neg Bx															
	Pos Bx															
	TAHN															

	Tumor		0.10								0.09
22	**Neg Bx**										
	Pos Bx										
	TAHN										
	Tumor			0.02							
23	**Neg Bx**										
	Pos Bx										
	TAHN										
	Tumor										
24	**Neg Bx**										
	Pos Bx										
	TAHN										
	Tumor									0.15	
25	**Neg Bx**										
	Pos Bx										
	TAHN										
	Tumor										
26	**Neg Bx**										
	Pos Bx										
	TAHN										
	Tumor							0.05			
27	**Neg Bx**										
	Pos Bx										
	TAHN										
	Tumor										
28	**Neg Bx**										
	Pos Bx										
	TAHN										
	Tumor										
29	**Neg Bx**										
	Pos Bx										
	TAHN										
	Tumor										
30	**Neg Bx**										
	Pos Bx										
	TAHN										
	Tumor										
31	**Neg Bx**										
	Pos Bx										
	TAHN										
	Tumor	0.06									
32	**Neg Bx**										
	Pos Bx										
	TAHN										
	Tumor										

consistent from case to case of prostate cancer. Viewed from the perspective that the entire genome becomes unstable during carcinogenesis, the assay employed by our laboratory reflects genome-wide genomic instability as opposed to locus-specific instability. Additionally, our assay avoids the requirement of a 'normal' control sample, reducing the amount of tissue or other biologic samples required from the patient, and permitting evaluation of archival tissues where patient-matched normal tissue may not be available. Because the assay is PCR based, only a small amount if tissue is required, such as a biopsy needle core. Previous studies from our laboratory in both breast and prostate cancers have demonstrated the presence of a field of genetically altered cells surrounding the tumor as demonstrated by both altered TC and allelic imbalance (*17, 48*). Taken together, these results demonstrate that AI in histologically normal tissue from a cancerous prostate is indeed informative regarding genomic instability and the likelihood of cancerous alterations being present, and does demonstrate the presence of a field of altered cells is present. The current study confirmed this finding.

This is the first study to compare nonspecific sites of allelic imbalance in patient matched biopsy and prostatectomy specimens using the assay developed within our laboratory. AI was detected in both cancerous and histologically normal tissues from both biopsy and prostatectomy specimens. Moreover, the numbers of sites of AI exceeded those found in normal tissues and overlapped those found in cancers. These findings indicate two things: a) a field of genetically altered cells are present at the time of biopsy in cores determined to be histologically normal, and b) the number of sites of AI in both cancerous and histologically normal tissues from needle core biopsies is informative of a cancer diagnosis. However, it is important to point out that all of the patients in this

cohort went on to prostatectomy due to the presence of prostate cancer. We have not yet performed a comparable analysis of biopsies that did not result in a cancer diagnosis or that contained only BPH or PIN. Thus, the conclusions of this investigation must be viewed provisionally.

The interesting finding of this study arises from the finding of matched sites of AI in patient matched tissues, such as TAHN and tumor specimens and biopsy and prostatectomy specimens. These findings imply that the tumor cells may arise from a clone found in the field of histologically normal, though genetically altered cells. Further, these findings support the theory of clonal selection in cancer progression, evidenced by the maintenance of a cell population containing specific genomic alterations. We interpret instances in which site of AI were present in TAHN tissue but not in the matched Tumor tissue to reflect genetically altered clones that did not give rise to the tumor, *i.e.* clones that were not selected and constituted either a minority of the cell population or that were lost completely. Most intriguing was the finding of conserved sites of AI in all for specimens of a single case. The likelihood of conservation of a single site within all 4 specimens was determined to be 0.01% and 0.02% for the 2 cases, providing further evidence that AI maintenance is not attributable to chance alone. The intriguing finding of conserved sites of imbalance between samples supports the theory of clonality of cancer cells and their precancerous progenitors. The results suggest that the abnormal field of cells arise early, and eventually gives rise to the tumor, accumulating mutations over time.

References

(1)   Bostwick, D. G., Burke, H.B., Djakiew, D., Euling, S., Ho, S., Landolph, J.,

        Morrison, H., Sonawane, B., Shifflett, T., Waters, D.J., Timms, B. (2004)

        Human Prostate Cancer Risk Factors. *Cancer Supplement 101*, 2371-2490.

(2)   Isaacs, J. T. (1997) Molecular markers of prostate cancer metastasis.

        American Journal of Pathology 150, 1511-1521.

(3)   Meikle, A. W., Smith, J.A. (1990) Epidemiology of prostate cancer. *Urol Clin

        N Am 17*, 709-718.

(4)   Tricoli, J. V., Schoenfeldt, M., Conley, B.A. (2004) Detection of prostate

        cancer and predicting progression: current and future diagnostic markers.

        Clinical Cancer Research 10, 3943-3953.

(5)   Catalona, W. J. (1996) Clinical utility od measurements of free and total

        prostate specific antigen (PSA): a review. *Prostate 7s*, 64-69.

(6)   Djavan, B., Ravery, V., ZLOTTA, A., Dobronski, P., Dobrovits, M., Fakhari,

        M., Seitz, C., Susani, M., Borkowski, J., Boccon-Gibod, L., Schulman, C.C.,

        Marberger, M. (2001) Prospective Evaluation of Prostate Cancer Detected on

        Biopsies 1, 2, 3 and 4: When Should We Stop? *Journal of Urology 166*, 1679-

        1683.

(7)   Balmer, L. L., Greco, K.E. (2004) Prostate cancer recurrence fear: the

        prostate-specific antigen bounce. *Clinical Journal of Urological Nursing 8*,

        361-367.

(8)   Northouse, L. L., Mood, D.W., Montie, J.E., Sandler, H.M., Forman, J.D., Hussain, M., Pienta, K.J., Smith, D.C., Sanda, M.G., Kershaw, T. (2007) Living With Prostate Cancer: Patients' and Spouses' Psychosocial Status and Quality of Life. *Journal of Clinical Oncology 25*, Online.

(9)   Talcott, J. A. (2007) Prostate Cancer Quality of Life: Beyond Initial Treatment—and the Patient. *Journal of Clinical Oncology 25*, Online.

(10)   Bernards R, W. R. (2002) Metastasis Genes: A progression puzzle. *Nature 418*, 823.

(11)   Langley, R. R., Fidler, I.J. (2007) Tumor Cell-Organ Microenvironment Interactions in the Pathogenesis of Cancer Metastasis. *Endocrine Reviews 28*, 297-321.

(12)   Chung, L. W. K., Baseman, A., Assikis, V., Zhau, H.E. (2005) Molecular insights into prostate cancer progression: the missing link of tumor microenvironment. *Journal of Urology 173*, 10-20.

(13)   Lengauer C., K. K. W., Vogelstein B. (1997) Genetic instability in colorectal cancers. *Nature 386*, 623-627.

(14)   Lengauer C., K. K. W., Vogelstein B. (1998) Genetic instabilities in human cancers. *Nature 396*, 643-649.

(15)   De Wever O, M. M. (2003) Role of tissue stroma in cancer cell invasion. *Journal of pathology 200*, 429-447.

(16)   Leman, E. S., Cannon, G.W., Trock, B.J., Sokoll, L.J., Chan, D.W., Mangold, L., Partin, A.W., Getzenberg, R.H. (2007) EPCA-2: A highly specific serum marker for prostate cancer. *Urology 69*, 714-20.

(17)   Heaphy CM, B. M., Fordyce CA, Haaland CM, Hines WC, Joste NE, Griffith

JK. (2006) Telomere DNA content and allelic imbalance demonstrate field

cancerization in histologicalle normal tissue adjacent to breast tumors.

International journal of cancer 119, 108-116.

(18)   Jero´nimo, C., Henrique, R., Hoque, M.O., Mambo, E., Ribeiro, F.R.,

Varzim, G., Oliveira, J., Teixeira, M.R., Lopes, C., Sidransky, D. (2004) A

Quantitative Promoter Methylation Profile of Prostate Cancer. *Clinical*

Cancer Research 10, 8472–8478.

(19)   Henrique, R., Jero´nimo, C., Teixeira, M.R., Hoque, M.O., Carvalho, A.L.,

Pais, I., Ribeiro, F.R., Oliveira, J.R., Lopes, C, Sidransky, D. (2006)

Epigenetic Heterogeneity of High-Grade Prostatic Intraepithelial Neoplasia:

Clues for Clonal Progression in Prostate Carcinogenesis. *Molecular Cancer*

Research 4.

(20)   Mehrotra J, V. S., Wang H, Chiu H, Vargo J, Gray K, Nagle RB, Neri JR,

Mazumder A. (2008) Quantitative, spatial resolution of the epigenetic field

effect in prostate cancer. *The prostate 68*, 152-160.

(21)   Dhir R, V. B., Arlotti J, Acquafondata M, Landsittel D, Masterson R,

Getzenberg RH. (2004) Early identification of individuals with prostate

cancer in negative biopsies. *The journal of urology 171*, 1419-1423.

(22)   Kwabi-Addo, B., Chung, C., Shen, L., Ittmann, M., Wheeler, T., Jelinek, J.,

Issa, J.J. (2007) Age-Related DNAMethylation Changes in Normal

Human Prostate Tissues. *Clinical Cancer Research 13*, 3796-3802.

(23)   Blackburn, E. H. (1991) Structure and function of telomeres. *Nature 350*, 569-573.

(24)   McEachern, M. J., Krauskopf, A, Blackburn, E.H. (2000) Telomeres and their control. *Annual Reviews Genetics 34*, 331-358.

(25)   Dang, C. (1999) c-Myc target gene involved in cell growth, apoptosis and metabolism. *Mol Cell Biol 19*, 1-11.

(26)   Kruk, P. A., N.J. Rampino, and V.A. Bohr. (1995) DNA damage and repair in telomeres: relation to aging. *Proc Nat'l Acad Sci, USA 92*, 258-262.

(27)   McClintock, B. (1941) The stability of broken ends of chromosomes in Zea mays. *Genetics 26*, 234-282.

(28)   McClintock, B. (1942) The fusion of broken ends of chromosomes following nuclear fusion. *Proc. Nat'l. Acad. Sci 28*, 458-463.

(29)   Vaziri, H. (1997) Critical telomere shortening regulated by the ataxia-telangiectasia gene acts as a DNA damage signal leading to activation of p53 protein and limited life-span of human diploid fibroblasts. A review. *Biochem. (Moscow) 62*, 1306-1310.

(30)   Wan TS, M. U., Poon SS, Tsao SW, Chan LC, Lansdorp PM. (1999) Absence or low number of telomere repeats at junctions of dicentric chromosomes. *Genes Chromosomes Cancer 24*, 83-86.

(31)   Evans, A. J. (2003) Alpha-methylacyl CoA racemase (P504S): overview and potential uses in diagnostic pathology as applied to prostate needle biopsy. *J Clin Path 56*, 892-897.

(32)   Filatov L, G. V., Hurt JC, Byrd LL, Phillips JM, Kaufmann WK. (1998)
         Chromosomal instability is correlated with telomere erosion and inactivation
         of G2 checkpoint function in human fibroblasts expressing human
         papillomavirus type 16 E6 oncoprotein. *Oncogene 16*, 1825-1838.

(33)   Nakayama M., G. M. L., Yegnasubramanian S., Lin X., DeMarzo A.M.,
         Nelson, W.G. (2004) GSTP1 CpG island hypermethylation as a molecular
         biomarker for prostate cancer. *J Cell Biochem 91*, 540-553.

(34)   Griffith, J. K., Bryant JE, Fordyce CA, Gilliland FD, Joste NE, Moyzis RK.
         (1999) Reduced telomere DNA content is correlated with genomic instability
         and metastasis in invasive human breast carcinoma. *Breast Cancer Res Treat
         54*, 59-64.

(35)   Petersen, S., Saretzki, G. von Zglinicki, T. (1998) Preferred accumulation of
         single-stranded regions in telomeres of human fibroblasts. *Exp Cell Res 239*,
         152-160.

(36)   von Zglinicki, T. (1998) Telomeres: influencing the rate of aging. *Ann NY
         Acad Sci 854*, 318-327.

(37)   Donaldson, L., Fordyce C, Gilliland F, Smith A, Feddersen R, Joste N,
         Moyzis R, Griffith J. (1999) Association between outcome and telomere DNA
         content in prostate cancer. *TheJournal of Urology 162*, 1788-92.

(38)   Fordyce, C. A., Heaphy, C.M., Joste, N.E., Smith, A.Y., Hunt, W.C., Griffith,
         J.K. (2005) Association Between Cancer-free Survival and Telomere DNA
         Content in Prostate Tumors. *The Journal of Urology 173*, 610-614.

(39) Fordyce, C. A., Heaphy, C.M., Griffith, J.K. (2002) Chemiluminescent Measurement of Telomere DNA Content in Biopsies. *BioTechniques 33*, 144-146, 148.

(40) Chandran UR, D. R., Ma C, Michalopoulos G, Becich M, Gilberston J. (2005) Differences in gene expression in prostate cancer, normal appearing prostate tissue adjacent to cancer and prostate tissue from cancer free organ donors. *BMC cancer 5*, 45.

(41) Barrett, T., Troup, D.B., Wilhite, S.E., Ledoux, P., Rudnev, D., Evangelista, C., Kim, I.F., Soboleva, A., Tomashevsky, M., Edgar, R. (2007) NCBI GEO: mining tens of millions of expression profiles—database and tools update. *Nucleic Acids Research 35*, D760-D765.

(42) Glinsky, G. V., Berezovska, O., Glinskii, A.B. (2005) Microarray analysis identifies a death-fromcancer signature predicting therapy failure in patients with multiple types of cancer. *Journal of Clinical Investigation 115*, 1503-1521.

(43) Hu, M., Cai, L., Bachman, K.E., van den Brule, F., Velculescu, V., Polyak, K. (2005) Distinct epigenetic changes in the stromal cells of breast cancers. *Nature Genetics 37*, 899-905.

(44) Pusztai, L. (2006) Chips to Bedside: Incorporation ofMicroarray Data into Clinical Practice. *Clinical Cancer Research 12*, 7209-7214.

(45) Skotheim RI, D. C., Kraggerud SM, Jakobsen KS, Lothe RA. (2001) Evaluation of loss of heterozygosity/allelic imbalance scoring in tumor DNA. *Cancer Genet Cytogenet 127*, 64-70.

(46) Sgueglia JB, G. S., Davis J. (2003) Precision studies using the ABI prism 3100 genetic analyzer for forensic DNA analysis. *Anal Bioanal Chem 376*, 1247-54.

(47) Bryant, J. E., Hutchings, K.G., Moyzis, R.K., Griffith, J.K. (1997) Measurement of Telomeric DNA Content in HUman Tissues. *BioTechniques 23*, 476-484.

(48) Heaphy, C. M., Hines, W.C., Butler, K.S., Haaland, C.M., Heywood, G., Fischer, E.G., Bisoffi M, Griffith, J.K. (2007) Assessment of the Frequency of Allelic Imbalance in Human Tissue Using a Multiplex Polymerase Chain Reaction System. *Jounral of Molecular Diagnostics 9*, 266-271.

(49) Hanson, J. A., Gillespie, J.W., Grover, A., Tangrea, M.A., and Chuaqui, R. F., Emmert-Buck, M.R., Tangrea, J.A., Libutti, S.K., Linehan, W.M., Woodson, K.G. (2006) Gene Promoter Methylation in Prostate Tumor-Associated Stromal Cells. *Journal of the National Cancer Institute 98*, 255-261.

(50) Harden, S. V., Tokumaru, Y., Westra, W.H., Goodman, S., Ahrendt, S.A., Yang, S.C., Sidransky, D. (2003) Gene Promoter Hypermethylation in Tumors and Lymph Nodes of Stage I Lung Cancer Patients. *Clinical Cancer Research 9*, 1370–1375.

(51) Smiaglia, D. J., Rush L.J., Frühwald, M.C., Dai, Z., Held, W.A., Costello, J.F., Lang, J.C., Eng, C, Li, B., Wright, F.A., Caligiuri, M.A., Plass, C. (2001) Excessive CpG island methylation in cancer cell lines versus primary human malignancies. *Human Molecular Genetics 10*, 1413-1419.

(52)   Esteller, M., Corn, P.G., Baylin, S. B., and Herman, J.G. (2001) A Gene Hypermethylation Profile of Human Cancer. *Cancer Research 61*, 3225-3229.

(53)   Li, L.-C., Okino, S.T., Dahiya, R. (2004) DNA methylation in prostate cancer. *Biochimica et Biophysica Acta 1704*, 87-102.

(54)   Clark, S. J. (2007) Action at a distance: epigenetic silencing of large chromosomal regions in carcinogenesis. *Human Molecular Genetics 16*, R88-R95.

(55)   Eads, C. A., Lord, R.V., Wickramasinghe, K., Long, T.I., Kurumboor, S.K., Bernstein, L., Peters, J.H., DeMeester, S.R., DeMeester, T.R., Skinner, K.A., Laird, P.W. (2001) Epigenetic Patterns in the Progression of Esophageal Adenocarcinoma. *Cancer Research 61*, 3410–3418.

(56)   Esteller, M., Guo, M., Moreno, V., Peinado, M.A., Capella, G., Galm, O., Baylin, S.B., Herman, J.G. (2002) Hypermethylation-associated Inactivation of the Cellular Retinol-Binding-Protein 1 Gene in Human Cancer. *Cancer Research 62*, 5902–5905.

(57)   Esteller, M. (2007) Epigenetic gene silencing in cancer: the DNA hypermethylome. *Human Molecular Genetics 16*, R50-R59.

(58)   Jero´nimo, C., Henrique, R., Hoque, M.O., Ribeiro, F.R., Oliveira, J., Fonseca, D., Teixeira, M.R., Lopes, C., Sidransky, D. (2004) Quantitative RARbeta2 Hypermethylation: A Promising Prostate Cancer Marker. *Clinical Cancer Research 10*, 4010-4014.

(59)   Perry, A. S., Foley, R., Woodson, K., Lawler, M. (2006) The emerging roles of DNA methylation in the clinical management of prostate cancer. *Endocrine-Related Cancer 13*, 357-377.

(60)   Rosenbaum, E., Hoque, M.O., Cohen, Y., Zahurak, M., Eisenberger, M.A., Epstein, J.I., Partin, A.W., Sidransky, D. (2005) Promoter Hypermethylation as an Independent Prognostic Factor for Relapse in Patients with Prostate Cancer Following Radical Prostatectomy. *Clinical Cancer Research 11*, 8321-8325.

(61)   Yates, D. R., Rehman, I., Abbod, M.F., Meuth, M., Cross, S.S., Linkens, D.A., Hamdy, F.C., Catto, J.W.F. (2007) Promoter Hypermethylation Identifies Progression Risk in Bladder Cancer. *Clinical Cancer Research 13*, 2046-2053.

(62)   Mehrotra, J., Varde, S., Wang, H., Chiu, H., Vargo, J., Gray, K., Nagle, R.B., Neri, J.R., Mazumder, A. (2008) Quantitative, spatial resolution of the epigenetic field effect in prostate cancer. *The prostate 68*, 152-160.

(63)   Nakayama, M., Gonzalgo, M.L., Yegnasubramanian, S., Lin, X., DeMarzo, A.M., Nelson, W.G. (2004) GSTP1 CpG island hypermethylation as a molecular biomarker for prostate cancer. *J Cell Biochem 91*, 540-553.

(64)   Chandran, U. R., Dhir, R., Ma, C., Michalopoulos, G., Becich, M., Gilberston, J. (2005) Differences in gene expression in prostate cancer, normal appearing prostate tissue adjacent to cancer and prostate tissue from cancer free organ donors. *BMC cancer 5*, 45.

(65)   Fraga, M. F., Esteller, M. (2002) DNA Methylation: A Profile of Methods and Applications. *Biotechniques 33*, 632-649.

(66)   Ding, S., Gong, B-D., Yu, J., Gu, J., Zhang, H-Y., Shang, Z-B., Fei, Q., Wang, P., Zhu, J.D. (2004) A Methylation profile of the promotor CpG islands of 14 "drug-resistance" genes in hepatocellular carcinoma. *World J Gastroenterol. 10*, 3433-3440.

(67)   Jiang, Z., Woda, B.A., Wu, C-L., Yang, X.J. (2004) Discovery and clinical application of a novel prostate cancer marker α-methylacyl CoA Racemase (P504S). *Anatomic Pathology 122*, 275-289.

(68)   Lee, T.-L., Leung, W.K., Chan, M.W.Y., Ng, E.K.W., Tong, J.H.M., Lo, K-W., Chung, S.C.S., Sung, J.J.Y., To, K-F. (2002) Detection of gene promoter hypermethylation in the tumor and serum of patients with gastric carcinoma. *Clinical Cancer Research 8*, 1761-1766.

(69)   Pellisé, M., Castells, A., Gine`s, A., Agrelo, R., Sole´, M., Castellvı´-Bel, S., Ferna´ndez-Esparrach, G., Llach, J., Esteller, M., Bordas, J.M., Pique, J.M. (2004) Detection of lymph node micrometastases by gene promoter hypermethylation in samples obtained by endosonography-guided fine-needle aspiration biopsy. *Cilinical Cancer Research 10*, 4444-4449.

(70)   Herman, J. G., Baylin, S.B. (1998) Methylation Specific PCR. *Current Protocols in Human Genetics*.

(71)   Braakhuis BJ, T. M., Kummer JA, Leemans CR, Brakenhoff RH. (2003) A genetic explanation of Slaughter's concept of field cncerization: evidence and clinical implications. *Cancer Research 63*, 1727-1730.

(72)   Ha PK, C. J. (2003) The molecular biology of mucosal field of the head and neck. *Crit Rev Oral Biol Med 14*, 363-369.

(73)   Slaughter DP, S. H., Smejkal W. (1953) Field cancerization in oral stratified squamous epithelium: clinical implications of multicentric origin. *Cancer 6*, 963-968.

(74)   Hockel M, D. N. (2005) The hydra phenomenon of cancer: why tumors recur locally after microscopically complete resection. *Cancer Research 65*, 2997-3002.

(75)   Dakubo GD, J. J., Birch-Machin MA, Parr RL. (2007) Clinical implications and utility of field cancerization. *Cancer cell international 7*.

(76)   Bostwick DG, S. A., Qian J, Darson M, Maihle NJ, Jenkins RB, Cheng L. (1998) Independant origin of multiple foci of prostatic intraepithelialneoplasia: comparison with matched foci of prostate carcinoma. *Cancer 83*, 1995-2002.

(77)   Collin SM, M. R., Metcalfe C, Gunnell D, Alberston PC, Neal D, Hamdy F, Stephens P, Lane JA, Moore R, Donovan J. (2008) Prostate cancer mortality in the USA and UK in 1975-2004: an ecological study. *The Lancet oncology 9*, 445-452.

(78)   McDavid K, L. j., Fulton JP, Tonita J, Thompson TD. (2004) Prostaet cancer incidence and mortality rates and trends in the United States and Canada. *Public Health Rep 119*, 174-186.

(79)   Rabbani F, S. N., Kava BR, Cookson MS, Fair WR. (1998) Incidence and
        clinical significance of false-negative sextant prostate biopsies. *The journal of
        urology 159*, 1247-1250.

(80)   Stamey, T. A. (1995) The central role of prostate specific antigen in diagnosis
        and progression of prostate cancer. *Journal of Urology 154*, 1418-9.

(81)   Christian JD, L. T., Morrow JF, Bostwick DG. (2005) Corpora amylacea in
        adenocarcinoma of the prostate: incidence and histology within needle core
        biopsies. *Modern patholgy 18*, 36-39.

(82)   Adamson ED, M. D. (2002) Egr-1 transcription factor: multiple roles in
        prostate tumor cell growth and survival. *Tumour Biol 23*, 93-102.

(83)   Eid MA, K. M., Iczkowski KA, Bostwick DG, Tindall DJ. (1998) Expression
        of early growth response genes in human prostate cancer. *Cancer Research
        58*, 2461-2468.

(84)   Thigpen AE, C. K., Guileyardo JM, Molberg KH, McConnell JD, Russell
        DW. (1996) Increased expression of early growth response-1 messenger
        ribonucleic acid in prostatic adenocarcinoma. *The journal of urology 155*,
        975-981.

(85)   Virolle T, K.-H. A., Baron V, De Gregorio G, Adamson ED, Mercola D.
        (2003) Egr-1 promotes growth and survival of prostate cancer cells.
        Identification of novel Egr-1 target genes. *The journal of biological chemistry
        278*, 11802-11810.

(86)   Baron V, D. S., Rhim J, Mercola D. (2003) Antisense to thhe early growth response-1 gene (Egr-1) inhibits prostate tumor development in TRAMP mice. *Annals of the New York Academy of Sciences 1002*, 197-216.

(87)   Baron V, D. G. G., Krones-Herzig A, Virolle T, Calogero A, Urcis R, Mercola D. (2003) Inhibition of Egr-1 expression reverses transformation of prostate cancer cells *in vitro* and *in vivo*. *Oncogene 22*, 4194-4202.

(88)   Adamson E, d. B. I., Mittal S, Wang Y, Hayakawa J, Korkmaz K, O'Hagan D, McClelland M, Mercola D. (2003) Egr-1 signaling in prostate cancer. *Cancer biology and therapy 2*, 617-622.

(89)   Mora GR, O. K., Mitchell RF, Jr., Jenkins RB, Tindall DJ. (2005) Regulation of expression of the early growth response gene-1 (EGR-1) in malignant and benign cells of thhe prostate. *The prostate 63*, 198-207.

(90)   Wlazlinski A, E. R., Hoffman MJ, Hader C, Jung V, Muller M, Schulz WA. (2007) Downregulation of several fibulin genes in prostate cancer. *The prostate 67*, 1770-1780.

(91)   Baron A, M. T., Tang D, Loda M. (2004) Fatty acid synthase: a metabolic oncogene in prostate cancer? *Journal of cellular biochemistry 91*, 47-53.

(92)   Kuhajda FP. (2006) Fatty acid synthase and cancer: new application of an old pathway. *Cancer Research 66*, 5977-5980.

(93)   Dhanasekaran SM, B. T., Ghosh D, Shah R, Varambally S, Kurachi K, Pienta KJ, Rubin MA, Chinnaiyan AM. (2001) Delineation of prognostic biomarkers in prostate cancer. *Nature 412*, 822-826.

(94) Kim JH, D. S., Mehra R, Tomlins SA, Gu W, Yu J, Kumar-Sinha C, Cao X, Dash A, Wang L, Ghosh D, Shedden K, Montie JE, Rubin MA, Pienta KJ, Shah RB, ChinnaiyanAM. (2007) Integrative analysis of genomic aberrations associated with prostate cancer progression. *Cancer Research 67*, 8229-8239.

(95) Luo JH. (2002) Gene expression alterations in human prostate cancer. *Drus today (Barc) 38*, 713-719.

(96) Xu J, S. J., Zhang X, Silva SJ, Houghton RL, Matsumura M, Vedvick TS, Leslie KB, Badaro R, Reed SG. (2000) Identification of differentially expressed genes in human prostate cancer using subtraction and microarray. *Cancer Research 60*, 1677-1682.

(97) Ernst T, H. M., Kenzelmann M, Cohen CD, Bonrouhi M, Weninger A, Klaren R, Grone EF, Wiesel M, Gudemann C, Kuster J, Schott W, Staehler G, Kretzler M, Hollstein M, Grone HJ. (2002) Decrease and gain of gene expression are equally discriminatory markers for prostate carcinoma: a gene expression analysis on total and microdissected prostate tissue. *The American journal of pathology 160*, 2169-2180.

(98) Tamura K, F. M., Tsunoda T, Ashida S, Takata R, Obara W, Yoshioka H, Daigo Y, Nasu Y, Kumon H, Konaka H, Namiki M, Tozawa K, Kohri K, Tanji N, Yokoyama M, Shimazui T, Akaza H, Mizutani Y, Miki T, Fujioka T, Shuin T, Nakamura Y, Nakagawa H. (2007) Molecular features of hormone-refractory prostate cancer cells by genome-wide gene expression profiles. *Cancer Research 67*, 5117-5125.

(99)   True L, C. I., Hawley S, Huang CY, Gifford D, Coleman R, Beer TM,

Gelmann E, Datta M, Mostaghel E, Knudsen B, Lange P, Vessella R, Lin D,

Hood L, Nelson PS. (2006) A molecular correlate to the Gleason grading

system for prostate adenocarcinoma. *Proceedings of the national academy of

sciences of the United States of America 103*, 10991-10996.

(100)   Setlur SR, R. T., Sboner A, Mosuera JM, Demichelis F, Hofer MD, Mertz

KD, Gerstein M, Rubin MA. (2007) Integrative microarray analysis of

pathways dysregulated in metastatic prostate cancer. *Cancer Research 67*,

10296-10303.

(101)   Braakhuis BJ, L. C., Brakenhoff RH. (2004) Using tissue adjacent to

carcinoma as a normal control: an obvious but questionable practice. *The

journal of pathology 203*, 620-621.

(102)   Yu YP, L. D., Jing L, Nelson J, Ren B, Liu L, McDonald C, Thomas R, Dhir

R, Finkelstein S, Michalopoulos G, Becich M, Luo JH. (2004) Gene

expression alterations in prostate cancer predicting tumor aggression and

preceding development of malignancy. *Journal of Clinical Oncology 22*, 2790-

2799.

(103)   Tuxhorn JA, A. G., Rowley DR. (2001) Reactive stroma in prostate cancer

progression. *The journal of urology 166*, 2472-2483.

(104)   Condon MS. (2005) The role of the stromal microenvironment in prostate

cancer. *Seminars in cancer biology 15*, 132-137.

(105)   Thiel G, C. G. (2002) Regulation of life and death by the zinc finger

transcription factor Egr-1. *Journal of cellular physiology 193*, 287-292.

(106) Khachigian LM, C. T. (1998) Early growth response factor 1: a pleiotropic mediator of inducible gene expression. *Journal of molecular medicine 76*, 613-616.

(107) Matthews CP, C. N., Young MR. (2007) AP-1 a target for cancer prevention. *Current cancer drug targets 7*, 317-324.

(108) Ozanne BW, S. H., McGarry LC, Hennigan RF. (2007) Transcription factors control invasion: AP-1 the first among equals. *Oncogene 26*, 1-10.

(109) Cheng I, K. L., Plummer SJ, Casey G, Witte JS. (2007) MIC-1 and IL!RN genetic variation and advanced prostate cancer risk. *Cancer epidemiology biomarkers Prev 16*, 1309-1311.

(110) Selander KS, B. D., Sequeiros GB, Hunter M, Desmond R, Parpala T, Risteli J, Breit SN, Jukkola-Vuorinen A. (2007) Serum macrophage inhibitory cytokine-1 concentrations correlate with the presence of prostate cancer bone metastases. *Cancer epidemiology biomarkers Prev 16*, 532-537.

(111) Huang CY, B. T., Higano CS, True LD, Vessella R, Lange PH, Garzotto M, Nelson PS. (2007) Molecular alterations in prostate carcinomas that associate with *in vivo* exposure to chemotherapy: identification of a cytopotective mechanism involving growth differentiation factor 15. *Clinical cancer research 13*, 5825-5833.

(112) Zhang T, K. V., Huez G, Gueydan C. (2002) AU-rich element-mediated translational control: complexity and multiple activities of trans-activating factors. *Biochemical society transactions 30*, 952-958.

(113)   Bouraoui Y, R. M., Garcia-Tunon I, Rodriguez-Berriguete G, Touffehi M,
        Rais NB, Fraile B, Paniagua R, Oueslati R, Royuela M. (2008) Pro-
        inflammatory cytokines and prostate-specific antigen in hyperplasia and
        human prostate cancer. *Cancer detection and prevention 32*, 23-32.

(114)   DeMarzo AM, N. W., Isaacs WB, Epstein JI. (2003) Pathological and
        molecular aspects of prostate cancer. *Lancet 361*, 955-964.

(115)   Suh J, R. A. (2004) NF-kappaB activation in human prostate cancer:
        important mediator or epiphenomenon? *Journal of cellular biochemistry 91*,
        100-117.

(116)   Menendez JA, M. I., Atlas E, Colomer R, Lupu R. (2004) Novel signaling
        molecules implicated in tumor-associated fatty acid synthase-dependant
        breast cancer cell proliferation and survival: role of exogenous dietary fatty
        acids, p53-p21WAF1/CIP1, ERK1/2 MAPK, p27KIP1, BRCA1, and NF-
        kappaB. *International journal of oncology 24*, 591-608.

(117)   Gallagher WM, C. C., Whelan LC. (2005) Fibulins and cancer: friend or foe?
        Trends in molecular medicine 11, 336-340.

(118)   Tanguay, S. (2000) The Role of complexed PSA and percent free PSA in
        prostate cancer detection. *Canadian Prostate Health Council 5*, 1.

(119)   Hanahan D., W. R. A. (2000) The Hallmarks of Cancer. *Cell 100*, 57-70.

(120)   Müller, I., Beeger, C., Alix-Panabières, C., Rebillard, X., Pantel, K.,
        Schwarzenbach, H. (2008) Identification of loss of heterozygosity on
        circulating free DNA in peripheral blood of prostate cancer patients:
        potential and technical improvements. *Clinical Chemistry 54*, 688-96.

(121) Lieberfarb, M. E., Lin, M., Lechpammer, M., Li, C., Tanenbaum, D.M., Febbo, P.G., Wright, R.L., Shim, J., Kantoff, P.W., Loda, M., Meyerson, M., Sellers, W.R. (2003) Genome-wide loss of heterozygosity analysis from laser capture microdissected prostate cancer using single nucleotide polymorphic allele (SNP) arrays and a novel bioinformatics platform dChipSNP. *Cancer Research 63*, 4781-5.